Oncogenic role of miR-183-5p in lung adenocarcinoma: A comprehensive study of qPCR, *in vitro* experiments and bioinformatic analysis

RONG-QUAN HE[1*], LI GAO[2*], JIE MA[1], ZU-YUN LI[2], XIAO-HUA HU[1] and GANG CHEN[2]

Departments of [1]Medical Oncology and [2]Pathology, First Affiliated Hospital of Guangxi Medical University, Nanning, Guangxi Zhuang Autonomous Region 530022, P.R. China

Received October 6, 2017; Accepted April 25, 2018

DOI: 10.3892/or.2018.6429

Abstract. Despite the fact that previous studies have reported the aberrant expression of miR-183-5p in lung adenocarcinoma (LUAD), the oncogenic role of miR-183-5p in LUAD and its underlying mechanisms have remained elusive. Hence, we attempted to elucidate the clinicopathological significance of miR-183-5p expression in LUAD and identify the biological function of miR-183-5p in LUAD in this study. Meta-analysis of Gene Expression Omnibus (GEO) data, data mining of The Cancer Genome Atlas (TCGA) and real-time quantitative polymerase chain reaction (qPCR) were performed to evaluate the clinicopathological significance of miR-183-5p in LUAD. Then, the effect of miR-183-5p on cell growth in LUAD was assessed by *in vitro* experiments. Additionally, the target genes of miR-183-5p were identified via miRWalk v.2.0 and TCGA. Gene Ontology (GO) analysis, Kyoto Encyclopedia of Genes and Genomes (KEGG) pathway analysis and Disease Ontology (DO) analysis were further carried out for the target genes. The targetability between target genes in key KEGG pathways and miR-183-5p was validated by independent samples t-test, Pearson's correlation test and immunohistochemistry results from the Human Protein Atlas (HPA). According to the results, miR-183-5p was overexpressed in LUAD and exhibited significant diagnostic value. Moreover, miR-183 expression was associated with tumor progression in the TCGA data. *In vitro* experiments revealed the positive influence of miR-183-5p on cell viability and proliferation as well as the negative effect of miR-183-5p on caspase-3/7 activity in LUAD, which supports the finding that target genes of miR-183-5p are mainly enriched in gene pathways containing cell adhesion molecules (CAMs) and gene pathways important in cancer. Therefore, we conclude that miR-183-5p acts as an oncogene in LUAD and participates in the pathogenesis of LUAD via the interaction networks of its target genes.

Correspondence to: Professor Xiao-Hua Hu, Department of Medical Oncology, First Affiliated Hospital of Guangxi Medical University, 6 Shuangyong Road, Nanning, Guangxi Zhuang Autonomous Region 530022, P.R. China
E-mail: gxmuhxh@163.com

Professor Gang Chen, Department of Pathology, First Affiliated Hospital of Guangxi Medical University, 6 Shuangyong Road, Nanning, Guangxi Zhuang Autonomous Region 530022, P.R. China
E-mail: chen_gang_triones@163.com

[*]Contributed equally

Key words: miR-183-5p, lung adenocarcinoma, Gene Expression Omnibus, real-time quantitative polymerase chain reaction, The Cancer Genome Atlas

Introduction

Lung cancer (LC) ranks highly on the list of lethal cancers, with 222,500 estimated new cases and 155,870 estimated deaths in the USA in 2017. Despite improvements in diagnosis and standard therapy, the prognosis of LC patients remains poor, with a 5-year survival rate of only 18% (1). Non-small cell lung cancer (NSCLC) accounts for a large proportion of all LC cases, and lung adenocarcinoma (LUAD) is the predominant histological type of NSCLC (2-4). An early diagnosis and effective therapy of LUAD is beneficial for the improved survival of LUAD patients. Thus, an understanding of the molecular mechanisms of LUAD and a valid biomarker for LUAD are urgently needed.

MicroRNAs (miRNAs) are small non-coding RNAs that suppress the translation or initiate the degradation of target mRNAs by perfectly or imperfectly binding to their 3'-untranslated regions (5). Currently, there is mounting evidence that miRNAs have vital functions in the occurrence and progression of a wide variety of cancers, with essential roles in diverse biological processes such as the proliferation, apoptosis, differentiation, drug resistance and metastasis of cancer cells (6-9). miR-183-5p, which belongs to the miR-183 family, is located at chromosome 7q32 with a high level of homogeneity (10). Previous studies have shown that aberrantly expressed miR-183-5p is involved in the progression of a wide variety of human cancers, including epithelial ovarian cancer, breast cancer and cervical cancer (11-13). Therefore, miR-183-5p has the potential to be a promising target for the effective diagnosis and therapy of cancers.

Several studies have also focused on miR-183-5p in LUAD. miR-183-5p was reported to be overexpressed in LUAD and to correlate with the tumor progression as well as poor prognosis of LUAD (14). In a study of Zhu *et al*, miR-183-5p exhibited a significant ability to distinguish between non-invasive and invasive LUAD (15). An *in vitro* study by Zhu *et al* declared that miR-183-5p targets PTPN4 to promote the migratory and invasive capacity of LUAD cells (16). Despite these previous findings, there is an overall lack of evaluation of the clinicopathological significance of miR-183-5p in LUAD, and the molecular mechanisms underlying its role remain unclear. Therefore, the present study aimed to explore miR-183-5p expression in LUAD and the diagnostic as well as prognostic significance of miR-183-5p in LUAD using the combined methods of Gene Expression Omnibus (GEO) meta-analysis, data retrieval from The Cancer Genome Atlas (TCGA) and real-time quantitative polymerase chain reaction (qPCR). We also endeavored to clarify the molecular function of miR-183-5p in LUAD using *in vitro* experiments and bioinformatic analysis of the target genes.

Materials and methods

Investigation of miR-183-5p expression in LUAD based on GEO data

Searching strategies and inclusion or exclusion criteria. miR-183-5p expression in LUAD and non-cancer tissue data from GEO microarray chips were acquired from GEO (http://www.ncbi.nlm.nih.gov/geo/) using the following search strategies: (miRNA OR miR) AND (lung OR pulmonary) AND (cancer OR neoplasm).

The preliminary retrieval results were first selected by scanning the title and abstract. The reserved studies after the initial selection were further screened according to the established inclusion and exclusion criteria. Studies that met the following characteristics were eligible for the meta-analysis: i) the study included LUAD and non-cancer tissue samples; ii) the study provided expression values for miR-183-5p in LUAD and non-cancer tissues; and iii) the tissue samples in the study originated from humans. Studies were excluded if i) the study included tissue samples of only either LUAD or non-cancer tissues; ii) the study contained insufficient data on miR-183 expression in the tissue samples; and iii) the tissue samples in the study were not from humans.

Data extraction. The following information was extracted from the included GEO datasets to calculate an overall standardized mean difference (SMD): GSE ID, first author, publication year, country, experimental type, sample type, platform, number (N) of cases in cancer group, mean (M) ± standard deviation (SD) of miR-183-5p expression in cancer group, N of cases in the non-cancer group, and M±SD of miR-183-5p expression in the non-cancer group. To obtain the sensitivity, specificity and Youden index for the data elements, a summary receiver operating characteristic (SROC) curve was created, and a receiver operating characteristic (ROC) curve was created for each GSE dataset by SPSS v.22.0. True positivity (TP), false positivity (FP), false negativity (FN) and true negativity (TN) of each GSE dataset were calculated according to the maximum Youden index and the corresponding cut-off value.

GEO meta-analysis. The effect sizes of the selected studies were aggregated as the SMD with 95% confidence intervals (95% CI). Chi-square tests of Q and the I^2 statistic were employed for the evaluation of heterogeneity between included studies. A $P<0.05$ or an $I^2>50\%$ was considered as significant heterogeneity, which implied that a random-effect model should be applied to pool the effect sizes. Otherwise, a fixed-effect model was utilized to pool the effect sizes when $P>0.05$ or $I^2<50\%$ (17). Then, subgroup analysis was used to detect the source of heterogeneity based on the characteristics of the studies. The impact of a single study on the overall pooling results was evaluated by sensitivity analysis through omission of each study one at a time. Additionally, Begg's and Egger's tests were carried out to confirm whether publication bias existed in the studies.

To assess the overall diagnostic value of all the included GSE datasets as well as the diagnostic value of plasma miRNA, Meta-DiSc v.1.4 was employed to plot SROC curves based on the TP, FP, FN and TN value of all studies. Value for area under curve (AUC) value ranging from 0.5 to 1 was indicative of a diagnostic capacity from poor to superior, respectively (18).

TCGA data excavation. The clinicopathological significance of miR-183-5p expression in LUAD was further analyzed with expression data of miR-183-5p precursor miR-183 in LUAD downloaded from TCGA (https://cancergenome.nih.gov/). All statistical analysis of TCGA data was performed in SPSS v.22.0 and the expression value of miR-183 was presented in the form of M±SD. The difference of miR-183 expression in two different groups of clinicopathological parameters was evaluated by independent samples t-test. When there were three or more groups of clinicopathological parameters, the distribution difference of miR-183 expression was assessed by Kruskal-Wallis (K-W) test. The diagnostic significance of miR-183 in LUAD was estimated by ROC curves and the implications of AUC for diagnostic ability of miR-183 were the same as stated above. Additionally, all the LUAD patients were divided based on the average of miR-183 expression value, and Kaplan-Meier survival curves were utilized to measure the influence of miR-183 on the prognosis of LUAD patients. $P<0.05$ was considered significant.

Validation of the clinicopathological significance of miR-183-5p in LUAD using qPCR

Patients. A total of 101 LUAD tissues and paired non-cancer tissues (56 males and 45 females) processed with formalin fixation and paraffin embedding were collected from the First Affiliated Hospital of Guangxi Medical University (Nanning, China) during the period from January 2012 to February 2014. The study was approved by the Research Ethics Committee of the First Affiliated Hospital of Guangxi Medical University. Signed informed consents were acquired from all the LUAD patients prior to their involvement in this study.

qPCR. The extraction and normalization of RNA as well as qPCR was carried out as described in previous studies (19,20). The coding sequence of miR-183-5p as identified through TaqMan® MicroRNA Assays (cat. no. 4427975-000416; Applied Biosystems: Thermo Fisher Scientifi, Inc., Grand Island, NY, USA) was 000417, UGUAAACAUCCUCGA

CUGGAAG. A TaqMan® MicroRNA Reverse Transcription kit (4366596; Applied Biosystems: Thermo Fisher Scientifi, Inc.) was applied to perform the RT reactions in a 10-μl volume. An Applied Biosystems PCR 7900 instrument was utilized to conduct the PCR. All the experiments including blank controls were carried out in triplicate. The difference in miR-183-5p expression between LUAD and peripheral non-cancer tissues was evaluated with the method of $2^{-\Delta Cq}$.

Statistical analysis for qPCR. The statistical analysis for qPCR data was conducted in SPSS v.22.0. miR-183-5p expression in LUAD and non-cancer tissues was compared by paired samples t-tests and the subsequent analysis of the clinicopathological significance of miR-183-5p expression in LUAD was carried out as described in the TCGA data excavation section.

Integrated meta-analysis. To achieve an overall assessment of the clinicopathological significance of miR-183-5p in LUAD, we pooled all the expression and diagnostic data of miR-183-5p from included GSE datasets, extracted TCGA data and qPCR results to conduct an integrated meta-analysis. SMD and SROC were calculated from all the pooled studies. Then, subgroup analysis, sensitivity analysis and detection of publication bias were performed to identify the source of heterogeneity, as described above.

In vitro experiment

Cell transfections and qPCR. Three human NSCLC cell lines: H460, A-549 and H1299 were acquired from American Type Culture Collection (ATCC, Manassas, VA, USA) and were cultured in Dulbecco's modified Eagle's medium (DMEM) (Gibco; Thermo Fisher Scientific, Inc., Grand Island, NY, USA) containing 10% fetal bovine serum and penicillin-streptomycin at 37˚C under a humidified atmosphere of 5% CO_2. Each of the *in vitro* experiments was performed 3 times. Before transfection, LUAD cells were plated in 96-well plates at $2.5x10^3$ cells/well and maintained at 37˚C for 24 h. Blank control, negative mimic control, miR-183-5p mimic, negative inhibitor control and miR-183-5p inhibitor (Ambion; Thermo Fisher Scientific, Inc., Carlsbad, CA, USA) were transfected in LUAD cell lines at a final concentration of 60 nmol/l with Lipofectamine 2000 following the manufacturer's instructions. The concentration for transfections was determined based on previous studies (21,22). miR-183-5p expression was detected with qPCR in Applied Biosystems PCR 7900 system as stated previously (23-26).

Effect of miR-183-5p on the biological behaviors of LUAD cells. The impact of miR-183-5p on the proliferation, viability and apoptosis of LUAD cells was measured by fluorometric resorufin viability assays, MTS assays and Apo-ONE Homogeneous Caspase-3/7 assays, as described in previous studies (25,26).

Statistical analysis of in vitro experiments. Statistical analysis was carried out in SPSS v.22.0. All data are expressed in the form of M±SD. Two-way analysis of variance (ANOVA) and Bonferroni post-tests were used for the comparisons among groups. We defined P<0.05 as statistically significant.

Network analysis of the target genes

Acquisition of target genes. Target genes of miR-183-5p came from two sources: TCGA data and miRWalk v.2.0. Downregulated genes in LUAD were downloaded from TCGA and subsequently processed with an edgeR software package. Genes with a false discovery rate (FDR) value <0.05 were selected as potential target genes. Apart from TCGA, miRWalk v.2.0 was also applied to the data to predict the target genes. Genes that appeared in at least four of the 12 software programs from miRWalk v.2.0 were considered as the possible target genes. Then, overlapping genes in the recorded lists of potential target genes from TCGA and miRWalk v.2.0 were regarded as the reliable target genes of miR-183-5p in LUAD.

Gene Ontology (GO) and Kyoto Encyclopedia of Genes and Genomes (KEGG) pathway analysis. GO analysis and KEGG pathway analysis from the online tool Database for Annotation, Visualization and Integration Discovery (DAVID) were applied to analyze functional enrichment of the target genes as stated previously (27).

Disease Ontology (DO) analysis. The clustering of the target genes in human diseases was investigated by DO analysis, which was performed by R package: clusterProfiler. DO terms with both P and Q-value <0.05 were selected as the significant terms enriched by target genes.

Protein-protein interaction (PPI) networks. PPI networks for the key KEGG pathways of LUAD were created by Search Tool for the Retrieval of Interacting Genes (STRING)/Proteins v.10.0 with all the component genes. The relationships between proteins were established from the following four channels: i) protein interactions documented in the literature; ii) high-throughput experiments; iii) genomic analysis and prediction; and iv) studies of co-expression. Hub genes of each PPI network were confirmed by comparing the connectivity degrees of the nodes from each PPI network.

Verification of genes in key KEGG pathways as directly targeted by miR-183-5p. To further verify genes from key KEGG pathways as directly targeted by miR-183-5p, an independent samples t-test was conducted by SPSS v.22.0 to examine the differential expression of these genes in LUAD and non-cancer tissues from TCGA. GraphPad Prism v.5 was employed to perform a Pearson's correlation test for evaluating the correlation between miR-183 expression and expression of the genes from TCGA. Moreover, we downloaded immunohistochemistry results for these genes in LUAD and normal tissues from the Human Protein Atlas (HPA), a database integrating immunohistochemistry analysis of proteins in multiple human tissues and cancers (28), to confirm whether these genes were downregulated in LUAD tissues or not.

Results

Included GEO datasets. A total of 340 GEO datasets appeared after initial search and 84 GEO datasets were retained after scanning titles and abstracts (29-37). According to the selection criteria, a total of 13 GEO datasets with 469 LUAD tissues and 272 non-cancer tissues were eligible for the meta-analysis.

Table I. Basic information of all included GSE datasets.

ID	First author	Year of publication	Country	Experiment type	Sample type	Platform	Cancer (N)	Cancer (M)	Cancer (SD)	Non-cancer (N)	Non-cancer (M)	Non-cancer (SD)
GSE27486	Patnaik (29)	2011	USA	Non-coding RNA profiling by array	Plasma	GPL11432	66	2.368	0.313	44	0.121	2.011
GSE40738	Patnaik (30)	2012	USA	Non-coding RNA profiling by array	Plasma	GPL16016	45	2.156	0.726	56	2.150	0.636
GSE93300	Qu[a]	2017	China	Non-coding RNA profiling by array	Plasma	GPL21576	9	-5.618	1.490	4	-8.187	1.022
GSE14936	Seike (31)	2009	USA	Non-coding RNA profiling by array	Tissue	GPL8879	24	2.851	0.135	22	2.790	0.069
GSE19945	Yuichi[a]	2013	Japan	Non-coding RNA profiling by array	Tissue	GPL9948	4	2.515	1.535	8	-0.823	1.697
GSE25508	Nymark (32)	2011	Finland	Non-coding RNA profiling by array	Tissue	GPL7731	10	6.808	0.600	10	6.249	0.181
GSE47525	van Jaarsveld (33)	2013	Netherlands	Non-coding RNA profiling by array	Tissue	GPL17222	7	2.394	0.123	14	2.419	0.132
GSE48414	Bjaanaes (34)	2014	Norway	Non-coding RNA profiling by array	Tissue	GPL16770	154	0.069	1.268	20	-1.678	0.508
GSE51853	Arima (35)	2014	Japan	Non-coding RNA profiling by array	Tissue	GPL7341	76	-0.398	1.311	5	-3.789	0.234
GSE63805	Robles (36)	2015	USA	Non-coding RNA profiling by array	Tissue	GPL18410	32	7.026	1.095	30	5.557	0.498
GSE74190	Jin[a]	2015	China	Non-coding RNA profiling by array	Tissue	GPL19622	36	2.284	0.272	44	0.121	2.011
GSE77380	Yoshimoto[a]	2016	Japan	Non-coding RNA profiling by array	Tissue	GPL16770	3	4.497	0.990	12	-0.303	3.193
GSE29248	Ma (37)	2012	China	Non-coding RNA profiling by array	Tissue	GPL8179	3	1,647.510	3,669.657	3	303.461	534.985

[a]Unpublished data. N, number; M, mean; SD, standard deviation.

Table II. Diagnostic data of all included GSE datasets.

Author	ID	TP	FP	FN	TN
Patnaik (29)	GSE27486	20	20	2	3
Patnaik (30)	GSE40738	20	18	15	38
Qu[a]	GSE93300	8	0	1	4
Seike (31)	GSE14936	7	3	4	6
Yuichi[a]	GSE19945	4	2	0	6
Nymark (32)	GSE25508	7	1	3	9
van Jaarsveld (33)	GSE47525	3	5	4	9
Bjaanaes (34)	GSE48414	118	0	36	20
Arima (35)	GSE51853	74	0	2	5
Robles (36)	GSE63805	27	2	5	28
Jin[a]	GSE74190	36	3	0	41
Yoshimoto[a]	GSE77380	3	1	0	11
Ma (37)	GSE29248	1	0	2	3

[a]Unpublished data. TP, true positivity; FP, false positivity; FN, false negativity; TN, true negativity.

The summarization of the included studies is displayed in Tables I and II. Distribution of miR-183-5p between LUAD tissues and non-cancer tissues as well as the diagnostic value of miR-183-5p for LUAD in each GSE dataset are illustrated by scatter plots (Fig. 1) and ROC curves (Fig. 2).

Meta-analysis of GEO datasets. The pooled effect sizes from forest plots (Fig. 3A) indicated that miR-183-5p expression was significantly higher in LUAD tissues than in non-cancer tissues (SMD=1.24, 95% CI=0.76-1.72, I^2=82.7%, P<0.001) with considerable study heterogeneity. To trace the origin of this heterogeneity, subgroup and sensitivity analyses were performed. Subgroup analysis based on sample types failed to locate the source of heterogeneity due to the insignificant 95% CI for the plasma subgroup (95% CI=-0.25-2.53) (Fig. 3B). The results of sensitivity analysis shown in Fig. 4A revealed that no study caused obvious deviation from the overall results. Moreover, Begg's and Egger's tests detected no publication bias (P=0.807) (Fig. 4B). With regard to the diagnostic ability of miR-183-5p for LUAD, SROC curves generated from all the included GSE datasets reported an AUC value of 0.8776 (Fig. 4C). Separating GSE datasets sampling plasma miR-183-5p from all the included GSE datasets, we obtained a SROC curve with an AUC value of 0.6813 (Fig. 4D).

Clinicopathological significance of miR-183 expression in TCGA data. As shown in Table III, miR-183 expression was significantly higher in LUAD tissues (P<0.001) and patients <60 years of age (P=0.012) compared with the matched control groups. Nevertheless, no significant relationships could be established between miR-183 expression and other clinicopathological variables of LUAD including sex, T stage, number of nodes, number of metastases, pathological stage, anatomic-organ subdivision and tumor location. In addition, the results from ROC curves indicated that miR-183 expression showed high diagnostic value for LUAD (AUC=0.985,

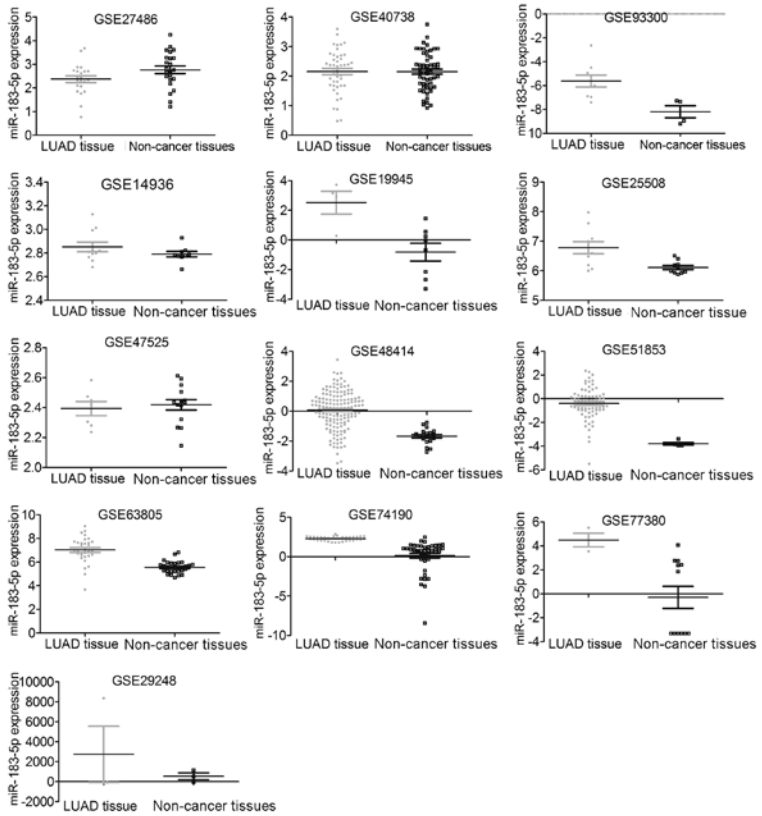

Figure 1. miR-183-5p expression in each of the included GSE datasets. The scatter plots display the differential expression levels of miR-183-5p in LUAD and non-cancer tissues for each of the included GSE datasets. LUAD, lung adenocarcinoma.

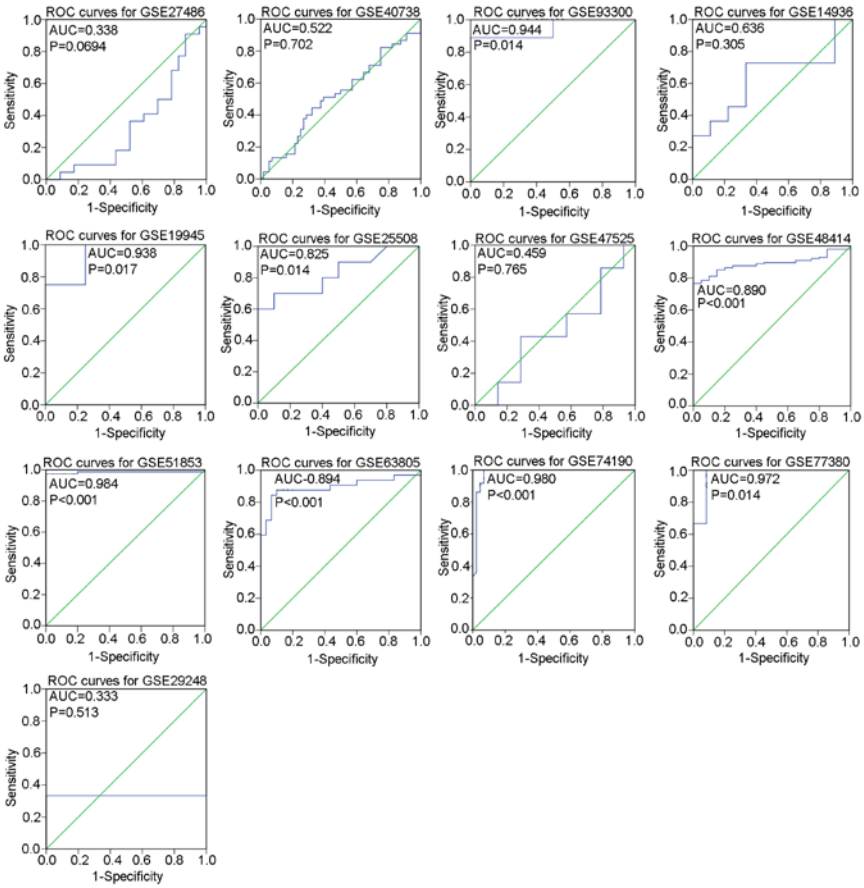

Figure 2. Diagnostic ability of miR-183-5p in LUAD for each of the included GSE datasets. A panel of ROC curves shows the diagnostic capacity of miR-183-5p for LUAD in each of the included GSE datasets. An AUC (area under the curve) value ranging from 0.5 to 1 was indicative of a diagnostic capacity from poor to superior, respectively. LUAD, lung adenocarcinoma; ROC, receiver operating characteristic; AUC, area under curve.

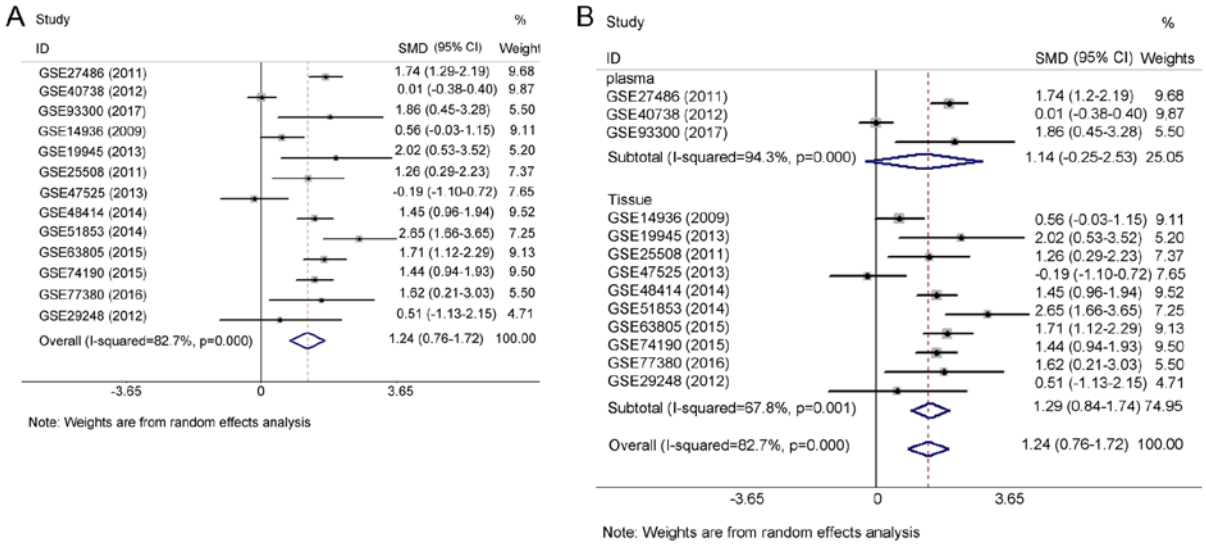

Figure 3. Forest plots for the GEO meta-analysis. (A) miR-183-5p presented markedly higher expression in LUAD tissues compared with non-cancer tissues (SMD=1.24, 95% CI=0.76-1.72, I^2=82.7%, P<0.001), with considerable study heterogeneity. (B) Subgroup analysis was conducted to assess the influence of the sample type on the heterogeneity of the studies. The pooled SMD for the plasma and tissue subgroups was 1.14 (-0.25-2.53) and 1.24 (0.76-1.72), respectively. Significant heterogeneity still existed in subgroups (I^2=94.3 and 67.8%). GEO, Gene Expression Omnibus; LUAD, lung adenocarcinoma; SMD, standardized mean difference.

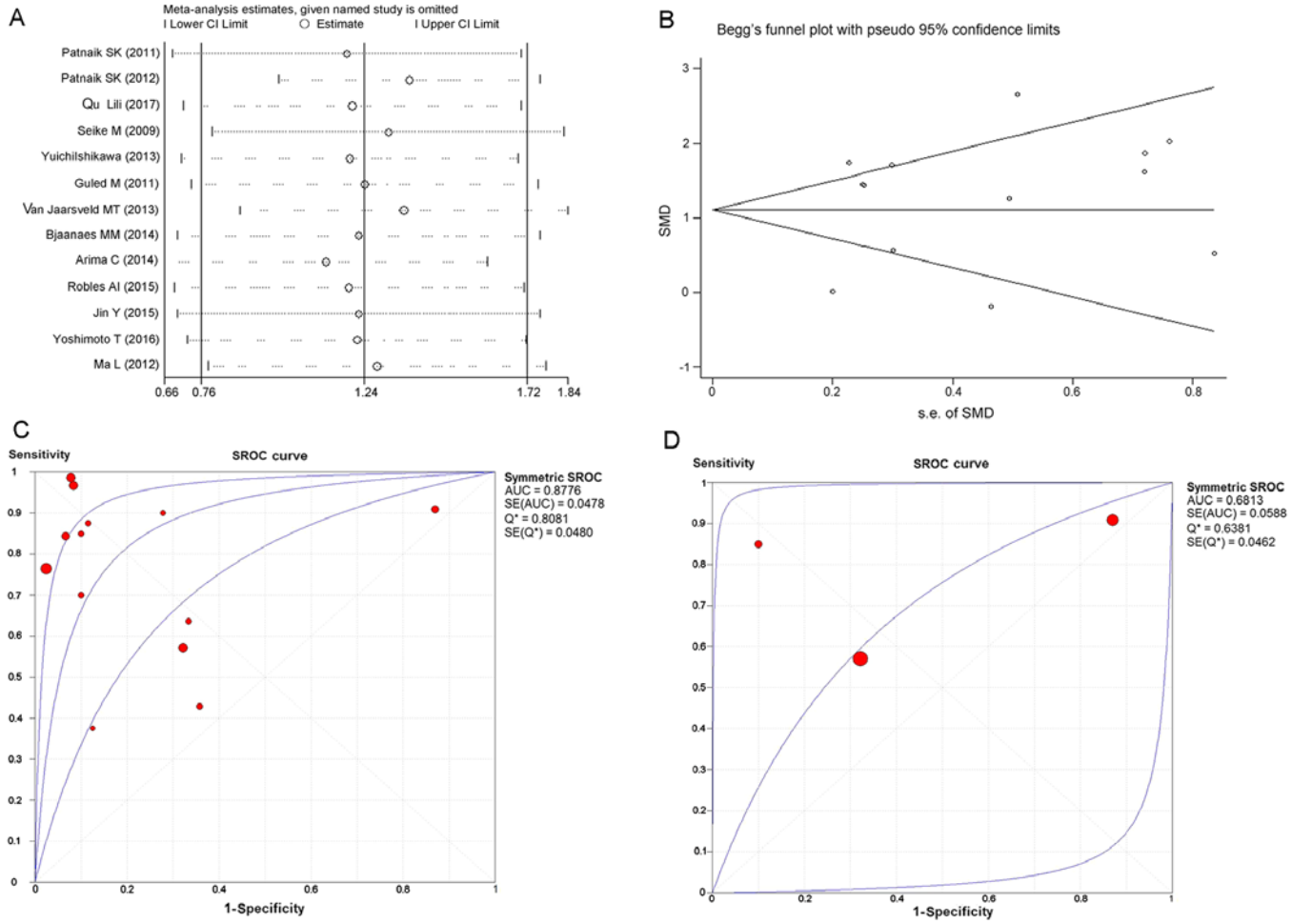

Figure 4. Sensitivity analysis, funnel plot and SROC curves for the GEO meta-analysis. (A) Sensitivity analysis for the GEO meta-analysis. No study caused obvious changes to overall results. (B) Funnel plot of publication bias for the GEO meta-analysis. The symmetrical funnel plot indicated no publication bias. (C) SROC curves for all the included GSE datasets. The AUC value of the SROC curves was 0.8776, indicating the significant diagnostic value of miR-183-5p in LUAD. (D) SROC curves for GSE datasets sampling plasma miR-183-5p. The AUC value of the SROC curves was 0.6813, indicating poor diagnostic value of miR-183-5p in LUAD. SROC, summary receiver operating characteristic; GEO, Gene Expression Omnibus; LUAD, lung adenocarcinoma; AUC, area under curve.

Table III. Relationship between miR-183 expression and clinicopathological parameters of LUAD from TCGA.

Clinicopathological feature	N	miR-183 relevant expression M±SD	t	P-value
Tissue				
Normal	46	10.661±0.572	25.544	<0.001
Lung cancer	441	13.180±1.072		
Age (years)				
≤60	199	13.317±1.150	2.531	0.012
>60	232	13.054±1.005		
Sex				
Female	234	13.166±1.082	0.288	0.774
Male	207	13.196±1.063		
T stage				
T1+T2	383	13.209±1.084	1.433	0.153
T3+T4	58	12.992±0.980		
Node				
No	288	13.155±1.092	-0.711	0.478
Yes	152	13.231±1.037		
Metastasis				
No	278	13.198±1.012	0.591	0.555
Yes	159	13.133±1.173		
Pathological stage				
I+II	346	13.155±1.084	-0.69	0.49
III+IV	90	13.242±1.023		
Anatomic-organ subdivision				
L_lower	69	13.042±0.990	3.159[a]	0.532
L_upper	105	13.170±1.085		
R_lower	84	13.129±1.057		
R_middle	18	13.226±0.913		
R_upper	154	13.268±1.132		
Location				
Peripheral	106	13.264±1.031	0.09	0.928
Central	54	13.248±1.082		

Independent samples t-test was performed to evaluate the relationship between miR-183 expression and the clinicopathological parameters of LUAD. [a]Kruskal-Wallis test was performed to assess the distribution difference of miR-183 in three or more groups of clinicopathological parameters. LUAD, lung adenocarcinoma; TCGA, The Cancer Genome Atlas; N, number; M, mean; SD, standard deviation.

P<0.001) (Fig. 5A). According to the log-rank test from Kaplan-Meier survival analysis, the influence of miR-183 on the prognosis of LUAD patients was not distinct (P>0.05) (data not shown).

Relationship between miR-183-5p expression and the clinicopathological features of LUAD from qPCR. A total of 101 LUAD and paired non-cancer tissues were taken from patients enrolled in our study. General information of the collected samples is listed in Table IV. From the results of the paired samples t-test, miR-183-5p expression was obviously higher in LUAD tissues (6.579±3.737) than in non-cancer

Table IV. Relationship between miR-183-5p expression and clinicopathological parameters of LUAD from qPCR data.

Clinical variable	N	miR-183-5p relevant expression M±SD	t	P-value
Tissue type				
LUAD	101	6.579±3.737	-2.103	0.038
Non-cancer	101	5.489±3.230		
Age (years)				
<60	41	6.556±3.613	-0.050	0.960
≥60	60	6.594±3.849		
Sex				
Female	45	7.063±3.865	-1.169	0.245
Male	56	6.190±3.618		
Smoke				
No	26	5.648±2.473	1.346	0.186
Yes	18	4.840±1.501		
Tumor size (cm)				
≤3	53	6.649±3.717	0.198	0.843
>3	48	6.501±3.796		
Lymph node metastasis				
No	45	5.605±2.746	-2.513	0.014
Yes	56	7.361±4.238		
Vascular invasion				
No	70	5.949±2.867	-2.151	0.038
Yes	31	8.002±4.962		
TNM				
I-II	45	5.605±2.746	-2.513	0.014
III-IV	56	7.361±4.238		
Pathological grading				
I	17	6.988±2.666	1.526[a]	0.466
II	61	6.305±3.767		
III	23	7.004±4.367		
EGFR amplification				
No	21	5.191±2.162	0.284	0.778
Yes	12	4.972±2.067		
EGFR protein expression				
Low	22	5.336±2.275	0.866	0.393
High	11	4.662±1.697		
EGFR mutation				
Wild-type	20	5.275±2.152	0.551	0.585
Mutation c	13	4.859±2.071		

Independent samples t-test was performed to evaluate the relationship between miR-183-5p expression and the clinicopathological parameters of LUAD. [a]Kruskal-Wallis test was performed to assess the distribution difference of miR-183-5p in three or more groups of clinicopathological parameters. LUAD, lung adenocarcinoma; qPCR, real-time quantitative polymerase chain reaction; N, number; M, mean; SD, standard deviation.

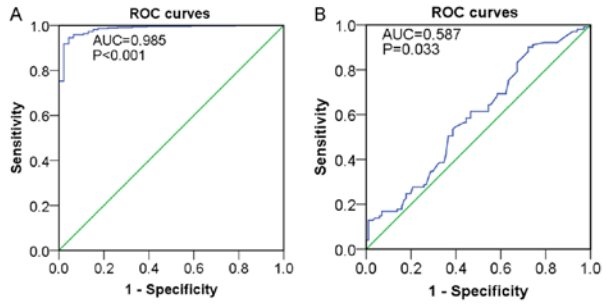

Figure 5. ROC curves for TCGA and qPCR data. (A) ROC curves for the TCGA data. The AUC value of the ROC curves was 0.985 (P<0.001), which reflected the strong diagnostic capacity of miR-183-5p for LUAD. (B) ROC curves for the qPCR data. The AUC value of the ROC curves was 0.587 (P=0.033), which was indicative of the potential diagnostic capacity of miR-183-5p in LUAD. ROC, receiver operating characteristic; TCGA, The Cancer Genome Atlas; qPCR, real-time quantitative polymerase chain reaction; AUC, area under curve; LUAD, lung adenocarcinoma.

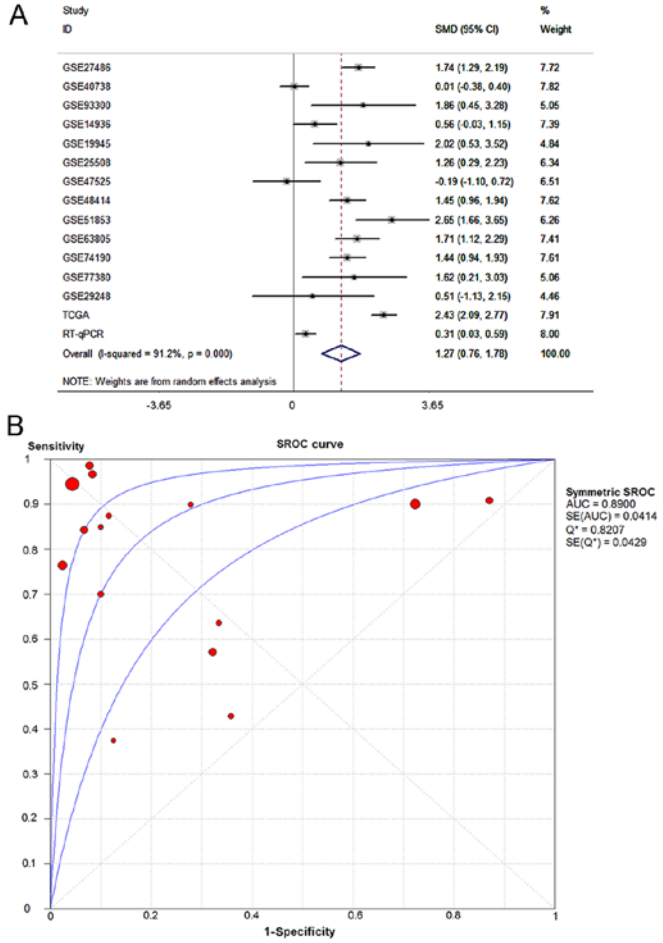

Figure 6. The forest plot and SROC curves for the integrated meta-analysis. (A) miR-183-5p showed markedly higher expression in LUAD tissues compared to in non-cancer tissues (SMD=1.27, 95% CI=0.76-1.78, I^2=91.2%, P<0.001), with considerable study heterogeneity. (B) The AUC value of the SROC curves was 0.8990, indicating the significant diagnostic value of miR-183-5p in LUAD. SROC, summary receiver operating characteristic; LUAD, lung adenocarcinoma; SMD, standardized mean difference; AUC, area under curve.

tissues (5.489±3.230) (P=0.038) (Table IV). Analysis from independent samples t-test suggested that patients with

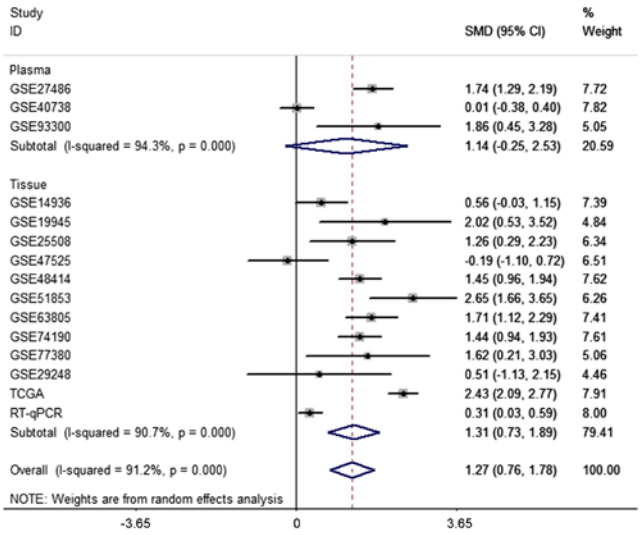

Figure 7. Forest plot of subgroup analysis for the integrated meta-analysis. Subgroup analysis was conducted to assess the influence of the sample type on the heterogeneity of the studies. The pooled SMD for the plasma and tissue subgroups was 1.14 (-0.25-2.53) and 1.31 (0.73-1.89), respectively. Significant heterogeneity still existed in the subgroups (I^2=94.3 and 90.7%). SMD, standardized mean difference.

lymph node metastasis, vascular invasion and advanced TNM stage (III-IV) exhibited higher miR-183-5p expression than patients without those features (P=0.014, 0.038, and 0.014). With respect to the diagnostic and prognostic value of miR-183-5p for LUAD, ROC curves revealed the potential diagnostic significance of miR-183-5p for LUAD (AUC=0.587, P=0.033) (Fig. 5B) while Kaplan-Meier survival analysis yielded no significant results supporting the role of miR-183-5p as an important prognostic factor for LUAD (log-rank P>0.05).

Integrated meta-analysis. The results of the integrated meta-analysis which contained a large sample with 1,011 LUAD tissues and 419 non-cancer tissues echoed with those from the GEO meta-analysis. miR-183-5p showed higher expression in LUAD tissues than in non-cancer tissues (SMD=1.27, 95% CI=0.76-1.78) (Fig. 6A). SROC curves with an AUC value of 0.890 demonstrated the significant diagnostic value of miR-183-5p for LUAD (Fig. 6B). Nevertheless, the results contained significant heterogeneity (I^2=91.2%, P<0.001). Further subgroup analysis and sensitivity analysis still failed to identify the origin of the heterogeneity (Figs. 7 and 8A). Apart from that, Begg's and Egger's test revealed that no publication bias existed among all the studies analyzed (P=0.882) (Fig. 8B).

Results from in vitro experiments. Transfection efficiency of miR-183 mimic and inhibitor was monitored by qPCR. miR-183-5p expression level increased 8- to 12-fold in all the three cell lines at 96 h post-transfection with the miR-183 mimic. At 96 h after transfection with the miR-183 inhibitor, 55-85% miR-183 knockdown was observed in all the three cell lines (Fig. 9A and B). As illustrated in Fig. 9C-E, cell viability evaluated by fluorometric resorufin viability assay increased slightly at 48 h in the H460, A459 and H1299 cells

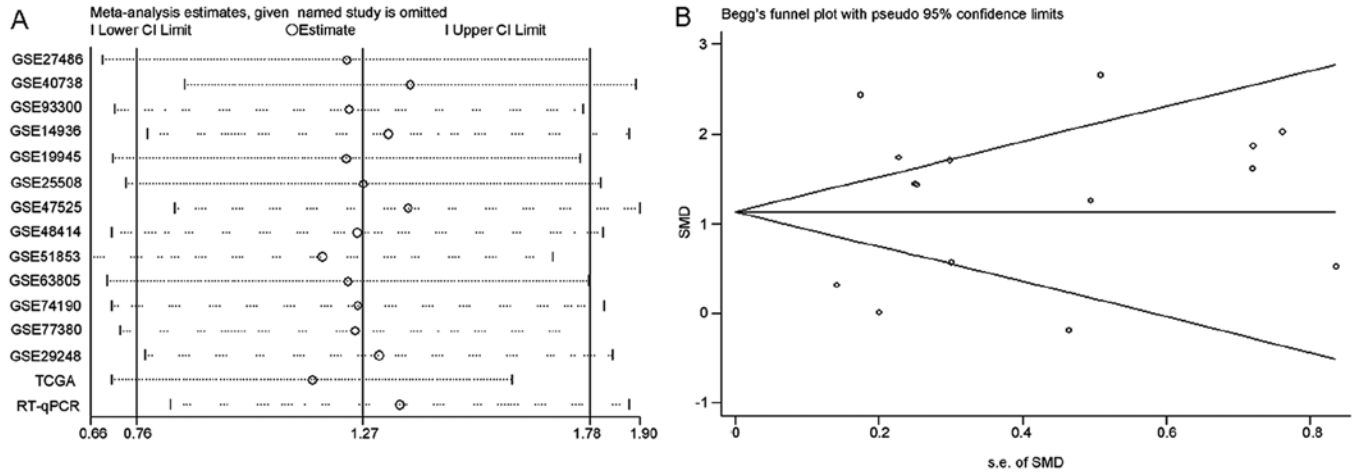

Figure 8. Sensitivity analysis and funnel plot for the integrated meta-analysis. (A) Sensitivity analysis for the integrated meta-analysis. No study caused obvious changes to the overall results. (B) Funnel plot of publication bias for the integrated meta-analysis. The symmetrical funnel plot indicated no publication bias. SMD, standardized mean difference.

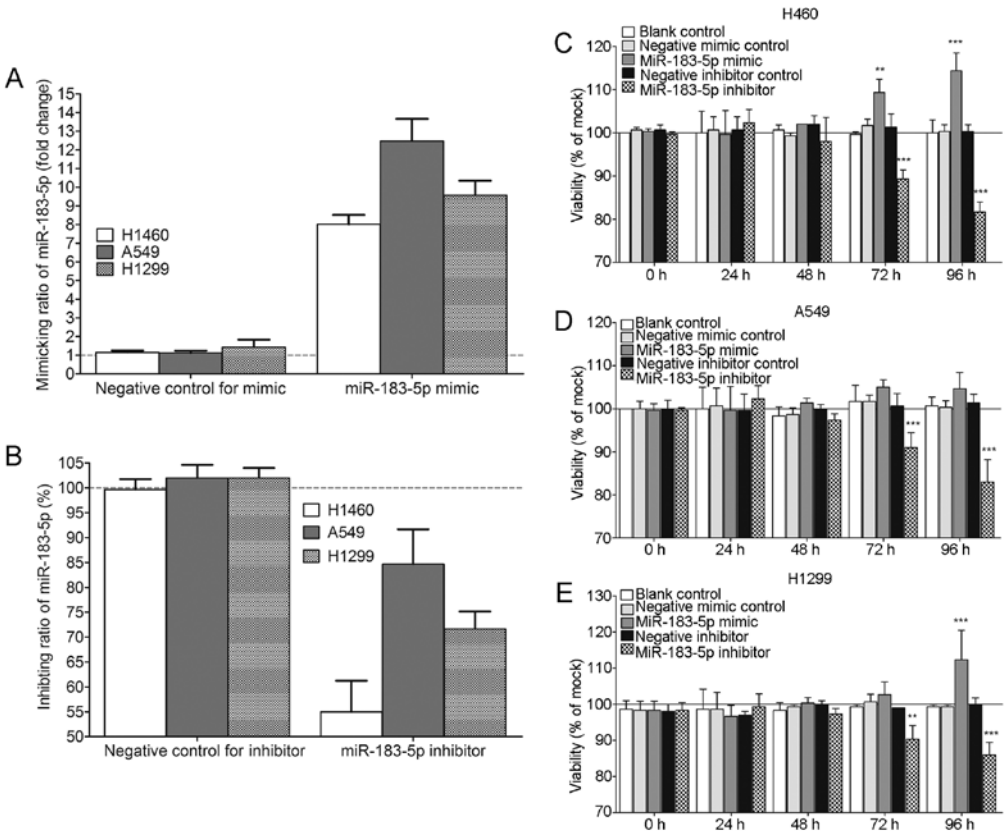

Figure 9. Transfection efficiency of miR-183 mimic and inhibitor plus the influence of miR-183-5p on cell viability of the tested cell lines. Transfection efficiency of miR-183 (A) mimic and (B) inhibitor in H460, A549 and H1299 cell lines. Influence of miR-183-5p on the cell viability of (C) H460, (D) A549 and (E) H1299 cell lines. Columns and bars represent the average of three repeated experiments and the SD, respectively. **P<0.01 and ***P<0.001. Comparisons were conducted between the miR-183-5p mimic or inhibitor groups and the corresponding negative or blank groups at the same time-point. SD, standard deviation.

transfected with the miR-183-5p mimic. The influence of miR-183-5p mimic on cell viability was observed to be most significant in H460 cells, in which cell viability was clearly increased compared to that of the blank control and negative mimic control at 72 h (P<0.01) and 96 h (P<0.001) (Fig. 9C). In A549 cell lines, cell viability in the miR-183-5p mimic group was higher than in the blank control and the negative mimic control at 72 and 96 h, although without statistical significance (P>0.05) (Fig. 9D). In the H1299 cell line, there was a sharp rise in the cell viability of the miR-183-5p mimic group at 96 h (P<0.001) (Fig. 9E). In contrast, all the column diagrams in Fig. 9 reflect a downward trend in cell viability after 48 h post-transfection with miR-183-5p inhibitor. In all three tested cell lines, cell viability decreased substantially

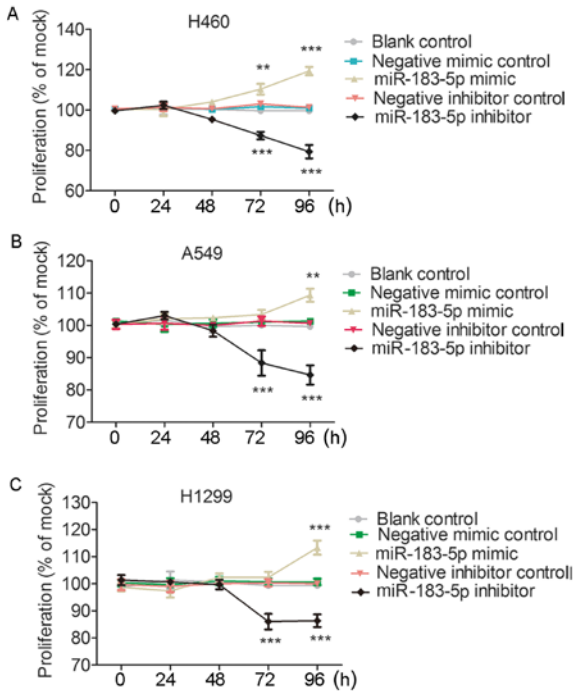

Figure 10. Influence of miR-183-5p on cell proliferation of the tested cell lines. (A) H460 cell lines. (B) A549 cell lines. (C) H1299 cell lines. Points and bars represent the average of three repeated experiments and the SD, respectively. **P<0.01 and ***P<0.001. Comparisons were conducted between the miR-183-5p mimic or inhibitor groups and the corresponding negative or blank groups at the same time-point. SD, standard deviation.

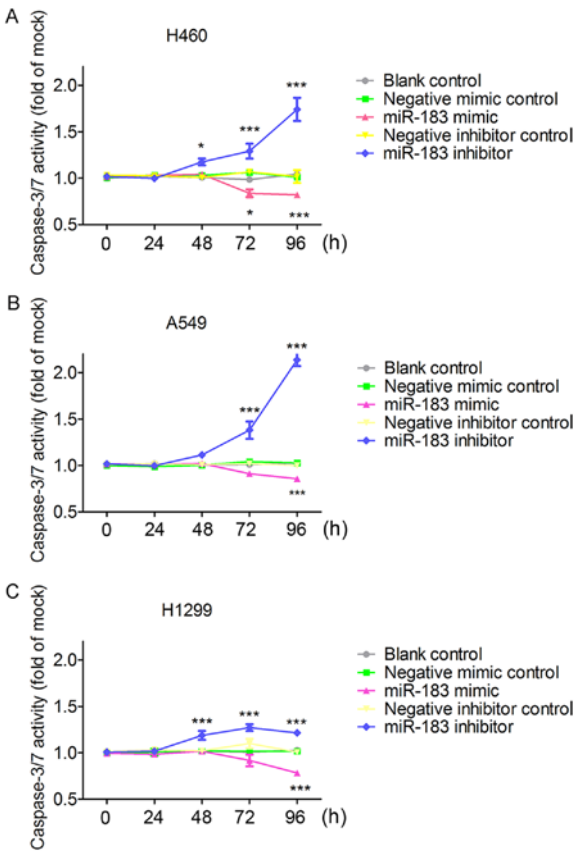

Figure 11. Effect of miR-183-5p on cell apoptosis of the tested cell lines. (A) H460 cell lines. (B) A549 cell lines. (C) H1299 cell lines. Points and bars represent the average of three repeated experiments and the SD, respectively. *P<0.05 and ***P<0.001. Comparisons were conducted between the miR-183-5p mimic or inhibitor groups and the corresponding negative or blank groups at the same time-point. SD, standard deviation.

in the miR-183-5p inhibitor group at 72 h (All P<0.01) and 96 h (All P<0.001) compared with in the blank control and the negative inhibitor control (Fig. 9). For the influence of miR-183-5p on cell proliferation, MTS assays reflected almost the same effect of miR-183-5p on cell growth as the fluorometric resorufin viability assay (Fig. 10). With regard to the effect of miR-183-5p on cell apoptosis, results from Apo-ONE Homogeneous Caspase-3/7 assays showed that the increase in caspase-3/7 activity started at 48 h in the miR-183 inhibitor group and the decline of caspase-3/7 activity started at 72 h in the miR-183 mimic group. Particularly, caspase-3/7 activity was significantly enhanced (P<0.001) at 72 and 96 h in miR-183-5p inhibitor group on the basis of the blank control and negative inhibitor group (Fig. 11), which was unanimously observed in all the three tested cells. Conversely, in the miR-183-5p mimic group, caspase-3/7 activity was significantly reduced on the basis of the blank control (P<0.001) and negative mimic control (P<0.05) in all the three tested cell lines (Fig. 11). In all the three assays, miR-183-5p stimulated cell growth and suppressed cell apoptosis in a time-dependent (Figs. 9-11) and dose-dependent (data not shown) manner.

Network analysis of target genes. According to the TCGA data analysis, a total of 2,609 downregulated genes with an FDR value <0.05 were identified as potential target genes of miR-183-5p. From the predictions of miRWalk v.2.0, a total of 5,065 genes occurred in at least four of the 12 online software programs. Taking genes that were found from both analyses, we obtained 432 reliable target genes of miR-183-5p in LUAD.

The selected target genes were further refined by GO and KEGG pathway analysis in DAVID. As shown in Table V, these target genes were most significantly enriched in the following terms of biological processes (BP): positive regulation of gene expression, cell adhesion and actin filament organization. With respect to cellular component (CC), the top three terms gathered by these target genes were plasma membrane, integral component of plasma membrane and receptor complex. These target genes were also significantly clustered in terms of molecular function (MF), such as Ras guanyl-nucleotide exchange factor activity, glycosaminoglycan binding and calcium ion binding. Three GO maps (Figs. 12-14) illustrate the functional interactions of the target genes. With regard to KEGG pathway analysis, the four most significant signaling pathways for the target genes of miR-183-5p were cell adhesion molecules (CAMs) and pathways in cancer, endocytosis and axon guidance (Table VI). The interactions between component genes of the four most significant pathways are displayed in four PPI networks (Fig. 15). A total of 10 genes including *CD34*, sialophorin (*SPN*), *WNT3A*, *FGFR2*, *WNT2B*, *PDGFB*, *AVPR2*, *VIPR1*, *PTGER4* and *ADCYAP1R1* were selected as the hub genes based on their degrees of connectivity in corresponding PPI networks.

DO analysis by clusterProfiler revealed that the target genes were significantly associated with the following

Table V. GO analysis of the target genes.

Category	ID	Term	Count	%	P-value
GOTERM_BP_DIRECT	GO:0010628	Positive regulation of gene expression	21	4.872	1.66E-06
GOTERM_BP_DIRECT	GO:0007155	Cell adhesion	27	6.265	1.25E-05
GOTERM_BP_DIRECT	GO:0007015	Actin filament organization	10	2.320	2.90E-05
GOTERM_BP_DIRECT	GO:0007165	Signal transduction	47	10.905	9.06E-05
GOTERM_BP_DIRECT	GO:0010629	Negative regulation of gene expression	12	2.784	2.39E-04
GOTERM_BP_DIRECT	GO:0032870	Cellular response to hormone stimulus	7	1.624	4.46E-04
GOTERM_BP_DIRECT	GO:0009611	Response to wounding	8	1.856	4.71E-04
GOTERM_BP_DIRECT	GO:0001934	Positive regulation of protein phosphorylation	11	2.552	5.30E-04
GOTERM_BP_DIRECT	GO:0070374	Positive regulation of ERK1 and ERK2 cascade	13	3.016	5.39E-04
GOTERM_BP_DIRECT	GO:0050665	Hydrogen peroxide biosynthetic process	4	0.928	8.20E-04
GOTERM_CC_DIRECT	GO:0005886	Plasma membrane	146	33.875	2.38E-10
GOTERM_CC_DIRECT	GO:0005887	Integral component of plasma membrane	64	14.849	4.73E-08
GOTERM_CC_DIRECT	GO:0043235	Receptor complex	15	3.480	7.61E-07
GOTERM_CC_DIRECT	GO:0009986	Cell surface	32	7.425	1.20E-06
GOTERM_CC_DIRECT	GO:0005578	Proteinaceous extracellular matrix	19	4.408	2.74E-05
GOTERM_CC_DIRECT	GO:0030054	Cell junction	26	6.032	2.97E-05
GOTERM_CC_DIRECT	GO:0016021	Integral component of membrane	151	35.035	3.25E-05
GOTERM_CC_DIRECT	GO:0009897	External side of plasma membrane	16	3.712	7.45E-05
GOTERM_CC_DIRECT	GO:0001725	Stress fiber	7	1.624	0.001128084
GOTERM_CC_DIRECT	GO:0031674	I band	5	1.160	0.001440976
GOTERM_MF_DIRECT	GO:0005088	Ras guanyl-nucleotide exchange factor activity	11	2.552	2.01E-04
GOTERM_MF_DIRECT	GO:0005539	Glycosaminoglycan binding	5	1.160	5.23E-04
GOTERM_MF_DIRECT	GO:0005509	Calcium ion binding	30	6.961	9.67E-04
GOTERM_MF_DIRECT	GO:0004714	Transmembrane receptor protein tyrosine kinase activity	6	1.392	0.001299161
GOTERM_MF_DIRECT	GO:0008289	Lipid binding	11	2.552	0.001702358
GOTERM_MF_DIRECT	GO:0050431	Transforming growth factor β binding	4	0.928	0.004589053
GOTERM_MF_DIRECT	GO:0004896	Cytokine receptor activity	5	1.160	0.007406533
GOTERM_MF_DIRECT	GO:0008201	Heparin binding	10	2.320	0.008250718
GOTERM_MF_DIRECT	GO:0005248	Voltage-gated sodium channel activity	4	0.928	0.008762612
GOTERM_MF_DIRECT	GO:0005024	Transforming growth factor β-activated receptor activity	3	0.696	0.009159889

There was a total of 93, 34 and 23 significant (P<0.05) GO terms of BP, CC and MF, respectively. Top ten GO terms for BP, CC and MF are displayed in the Table. GO, Gene Ontology; BP, biological process; CC, cellular component; MF, molecular function.

Figure 12. GO map for biological process (BP.) The GO map for BP is composed of 27 nodes and 32 links. Each node represents a specific GO term of a BP (P<0.001) and links between nodes illustrate the interactions between GO terms of the BP. Nodes with darker color are regarded as more significant GO terms. GO, Gene Ontology.

Figure 13. GO map for cellular component (CC). The GO map for CC is composed of 42 nodes and 57 links. Each node represents a specific GO term of CC (P<0.05) and links between nodes illustrate the interactions between GO terms of the CC. Nodes with darker color are regarded as more significant GO terms. GO, Gene Ontology.

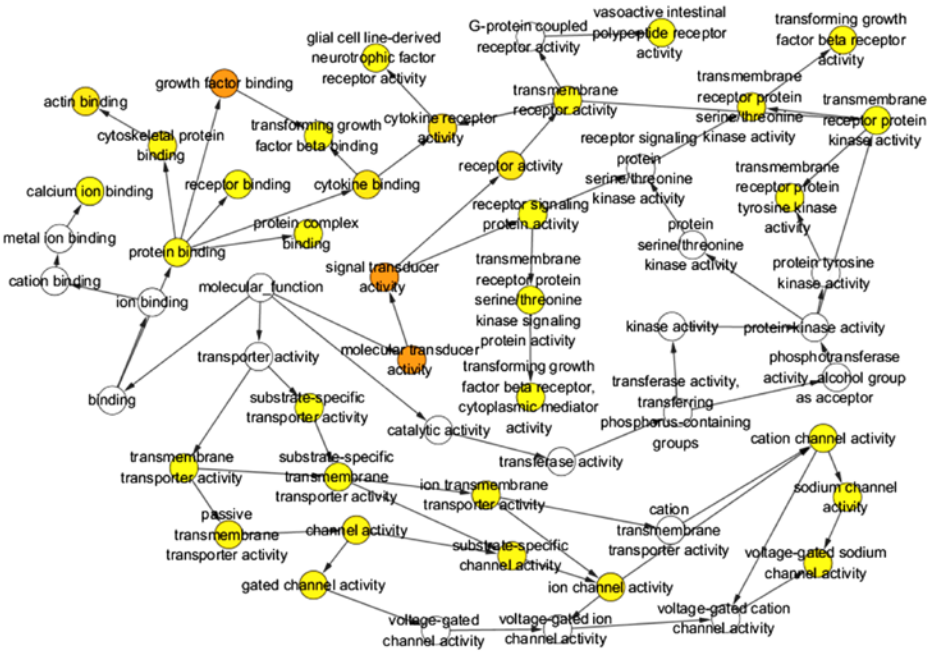

Figure 14. GO map for molecular funciton (MF). The GO map for MF is composed of 55 nodes and 68 links. Each node represents a specific GO term of MF (P<0.05) and links between nodes illustrate the interactions between GO terms of the MF. Nodes with darker color are regarded as more significant GO terms. GO, Gene Ontology.

diseases: migraine, Rett syndrome, chronic pulmonary heart disease and primary pulmonary hypertension (all P<0.05 and Q<0.05). (Table VII) (Fig. 16).

Verification of genes in key KEGG pathways as directly targeted by miR-183-5p. We conducted an independent samples t-test and Pearson's correlation test to validate the capabilities of miR-183-5p to target all the component genes in the CAM pathway. The results from the independent samples t-test suggested that expression of all these target genes was significantly lower in 535 LUAD tissues than in 59 non-cancer tissues (all P<0.001) (Fig. 17). Among the 11 component genes, five genes including *PECAM1*, *CDH5*, *SIGLEC1*, *CD34* and *CLDN18* showed significant correlation with miR-183-5p in LUAD (all P<0.05) (Fig. 18). Moreover, immunostaining evidence from the HPA database supported the downregulation of CD34 (antibody HPA036722), CADM1 (antibody CAB037266), PECAM1 (antibody HPA004690), SIGLEC1

Table VI. KEGG pathway analysis of the target genes.

Category	ID	Terms	Count	%	P-value
KEGG_PATHWAY	hsa04514	CAMs	11	2.552204176	0.001466545
KEGG_PATHWAY	hsa04550	Signaling pathways regulating pluripotency of stem cells	10	2.320185615	0.004641057
KEGG_PATHWAY	hsa05200	Pathways in cancer	18	4.176334107	0.008133914
KEGG_PATHWAY	hsa04080	Neuroactive ligand-receptor interaction	14	3.248259861	0.010639115
KEGG_PATHWAY	hsa00380	Tryptophan metabolism	5	1.160092807	0.012685346
KEGG_PATHWAY	hsa04924	Renin secretion	6	1.392111369	0.015130907
KEGG_PATHWAY	hsa04670	Leukocyte transendothelial migration	8	1.856148492	0.018169594
KEGG_PATHWAY	hsa04360	Axon guidance	8	1.856148492	0.026015978
KEGG_PATHWAY	hsa04144	Endocytosis	12	2.784222738	0.033890911
KEGG_PATHWAY	hsa04024	cAMP signaling pathway	10	2.320185615	0.037334507
KEGG_PATHWAY	hsa04060	Cytokine-cytokine receptor interaction	11	2.552204176	0.037626628
KEGG_PATHWAY	hsa04725	Cholinergic synapse	7	1.62412993	0.041290871
KEGG_PATHWAY	hsa04911	Insulin secretion	6	1.392111369	0.044616235

KEGG, Kyoto Encyclopedia of Genes and Genomes; CAMs, cell adhesion molecules.

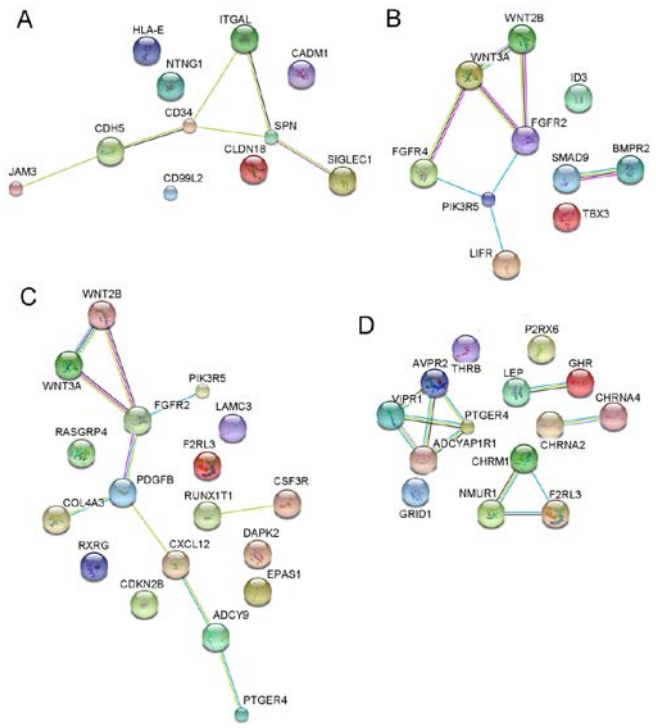

Figure 15. PPI networks for key KEGG pathways. PPI network for (A) the CAMs pathway (11 nodes and 9 edges), (B) the pathway in cancer pathway (10 nodes and 20 edges), (C) the endocytosis pathway (18 nodes and 22 edges) and (D) the axon guidance pathway (14 nodes and 29 edges). Nodes with different colors represent different component genes. Edges connecting nodes symbolize the interactions between component genes. PPI, protein-protein interaction; KEGG, Kyoto Encyclopedia of Genes and Genomes; CAMs, cell adhesion molecules.

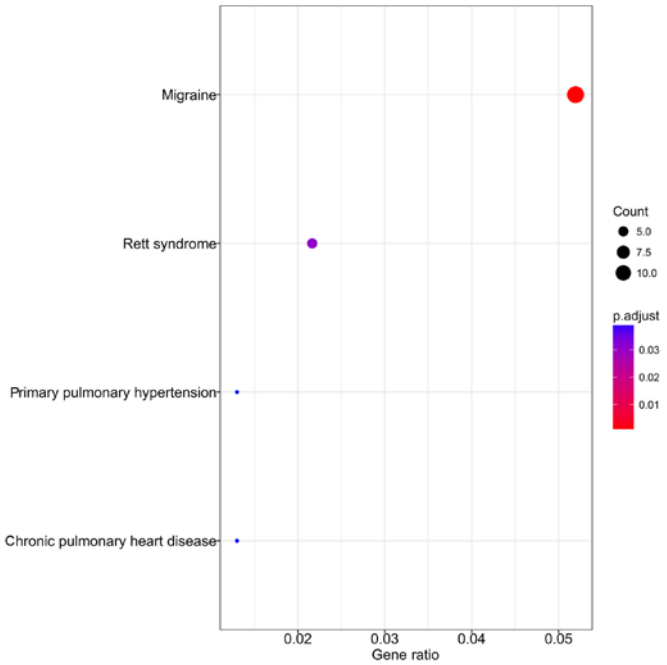

Figure 16. Dot plot for DO analysis. The dot plot describes the assembling of target genes in human disease. The vertical and horizontal axis represent the name of disease and the proportion of genes clustered in specific human disease, respectively. As the color of the dot changes from blue to red, the significance of the term increases. The size of the dot reflects the number of enriched genes. DO, Disease Ontology.

(antibody HPA053457) and SPN (antibody HPA055244) in LUAD tissues. Fig. 19 exhibits the immunostaining results of the five genes in normal and LUAD tissues. The staining intensity of the five genes was medium or strong in normal tissues, while low to non-existent in LUAD tissues.

Discussion

In this report, we used a combined method of GEO meta-analysis, TCGA data mining, qPCR, integrated meta-analysis, *in vitro* experiments and bioinformatic analysis of the target genes to comprehensively investigate the clinicopathological significance of miR-183-5p in LUAD and its underlying molecular basis. The results from this report revealed that overexpressed miR-183-5p had considerable diagnostic value in LUAD and was associ-

Table VII. DO analysis of the target genes.

ID	Description	Gene ratio	Bg ratio	P-value	P-adjusted	Q-value	Gene ID	Count
DOID:6364	Migraine	12/231	73/8,007	9.69E-07	0.000671237	0.000583196	477/5241/3683/6532/1636/4842/1524/3949/3952/6323/627/358	12
DOID:1206	Rett syndrome	5/231	17/8,007	8.92E-05	0.030893672	0.026841619	3399/1959/3952/22854/627	5
DOID:12326	Chronic pulmonary heart disease	3/231	5/8,007	0.000227082	0.039342028	0.034181879	659/6532/1636	3
DOID:14557	Primary pulmonary hypertension	3/231	5/8,007	0.000227082	0.039342028	0.034181879	659/6532/1636	3

DO, Disease Ontology.

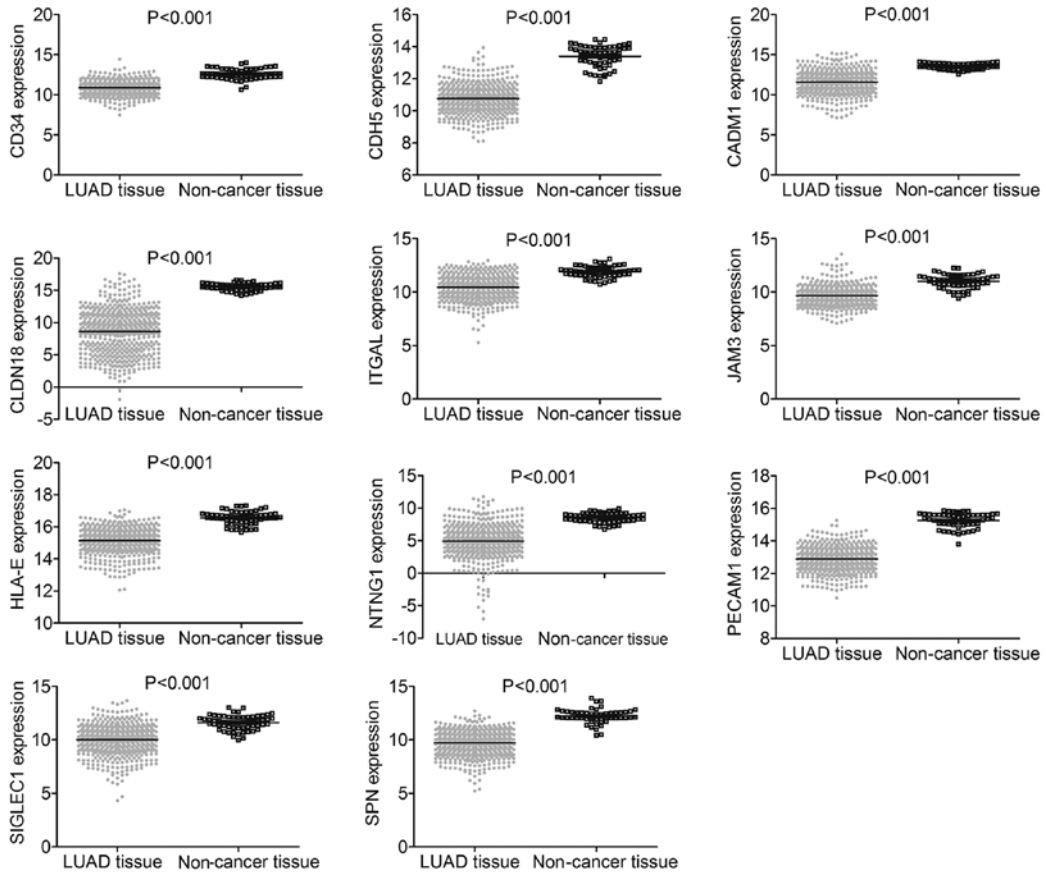

Figure 17. Expression of the component genes from the CAMs pathway in LUAD and non-cancer tissues. The scatter plots display the differential expression of the component genes from the CAMs pathway in LUAD and non-cancer tissues. All genes from the CAMs pathway were significantly downregulated in LUAD tissues (P<0.001). CAMs, cell adhesion molecules; LUAD, lung adenocarcinoma.

ated with the malignant progression of LUAD. Further *in vitro* experiments and bioinformatic analysis of the target genes of miR-183-5p showed the positive effect of miR-183-5p on cell growth in LUAD and revealed the specific biological processes and gene pathways common to miR-183-5p target genes, which may provide new insights into the oncogenesis of LUAD.

GEO meta-analysis, TCGA data mining, qPCR and the integrated meta-analysis in our study concordantly reported overexpression of miR-183-5p in LUAD tissues, which was in agreement with previous studies (38,39). The diagnostic value of miR-183-5p in LUAD was also studied. We found that miR-183-5p possessed strong diagnostic capacity for distinguishing LUAD tissues from non-cancer tissues via ROC curves derived from all the included GSE datasets, TCGA data mining and the integrated meta-analysis. ROC curves from qPCR also demonstrated the diagnostic potential of miR-183-5p for LUAD, although with weak statistical significance. The difference between ROC curves from all the included GSE datasets, TCGA data mining, qPCR and integrated meta-analysis might be explained by the type and number of samples. It should be

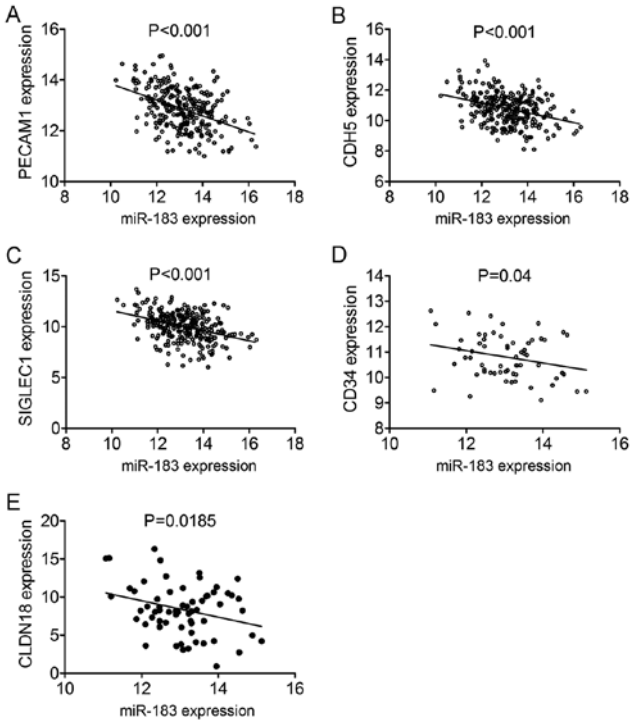

Figure 18. Pearson's correlation analysis of miR-183-5p expression and the expression of the component genes from the CAMs pathway. The correlation diagrams depict the correlations between miR-183-5p expression and the expression of component genes from the CAMs pathway. (A) *PECAM1* (P<0.001). (B) *CDH5* (P<0.001). (C) *SIGLEC1* (P<0.001). (D) *CD34* (P=0.04). (E) *CLDN18* (P=0.0185). Expression of *PECAM1*, *CDH5*, *SIGLEC1*, *CD34* and *CLDN18* showed significant correlation with miR-183-5p expression in LUAD. CAMs, cell adhesion molecules; LUAD, lung adenocarcinoma.

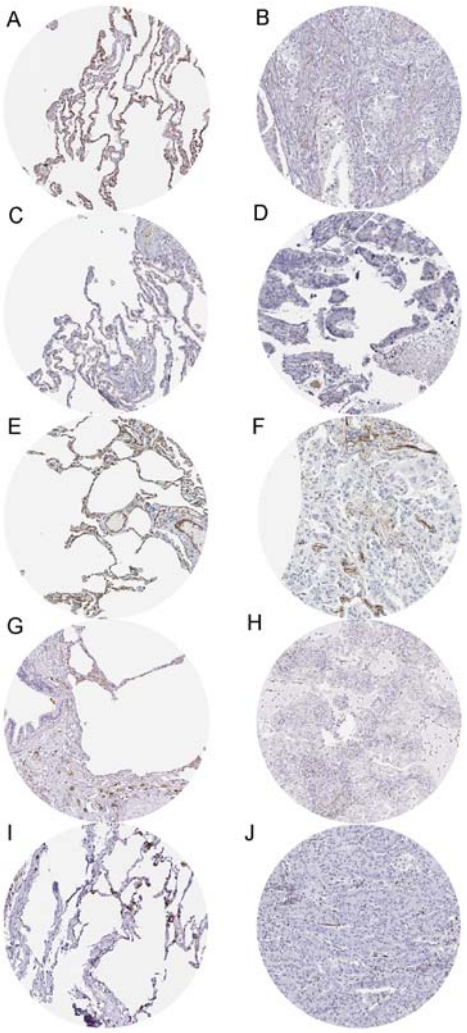

Figure 19. Immunohistochemistry of the component genes from the CAMs pathway in normal and LUAD tissues. CD34 expression in (A) normal and (B) LUAD tissues (antibody HPA036722). CADM1 expression in (C) normal and (D) LUAD tissues (antibody CAB037266). PECAM1 expression in (E) normal and (F) LUAD tissues (antibody HPA004690). SIGLEC1 expression in (G) normal and (H) LUAD tissues (antibody HPA053457). SPN expression in (I) normal and (J) LUAD tissues (antibody HPA055244). From the immunohistochemistry results of the HPA, all the above genes showed medium or high immunostaining in normal tissues. Conversely, low or no immunoreactivity of these genes was detected in LUAD tissues. CAMs, cell adhesion molecules; LUAD, lung adenocarcinoma; SPN, sialophorin; HPA, Human Protein Atlas.

noted that all the non-cancer tissues from qPCR were matched with the corresponding LUAD tissues, which is not the case in the GEO meta-analysis, the TCGA data mining or the integrated meta-analysis. Now that sensitive, less non-invasive biomarker was necessary for the early detection of LUAD, we singled out GSE datasets sampling plasma miR-183-5p to assess the diagnostic capacity of plasma miR-183-5p. Nevertheless, the results indicated a poorer diagnostic ability of plasma miR-183-5p in our study compared with miR-183-5p from both tissues and plasma. We conjectured that the less significant diagnostic ability of plasma miR-183-5p might be attributed to the lower levels of miR-183-5p in blood samples than in tissues, which is related to the phenomenon that LUAD cells in lung tissues assimilating exosomes containing miRNAs from the blood as a supplement of transcribed essential miRNAs (40-42). Considering the results of all the diagnostic evaluations, we are optimistic about the prospect of miR-183-5p as a diagnostic target for LUAD.

To investigate the role of miR-183-5p in the development of LUAD, we analyzed the relationship between miR-183-5p and the clinicopathological characteristics of LUAD. Given the positive correlation between miR-183-5p overexpression and lymph node metastasis, vascular invasion and advanced TNM stage in LUAD, it can be inferred that miR-183-5p may enhance the malignant properties of LUAD. To answer the question of how miR-183-5p affects the pathogenesis of LUAD, we conducted *in vitro* experiments to determine the influence of miR-183-5p on cell growth in LUAD.

As suggested by fluorometric resorufin viability assay and MTS assay, the proliferative ability of LUAD cells was augmented by miR-183-5p. The promotion of tumor cell growth by miR-183-5p has also been shown in *in vitro* experiments with pediatric acute myeloid leukemia, tongue squamous cell carcinoma and endometrial cancer (43-46). To ascertain whether the knockdown of miR-183-5p caused apoptosis or just inhibited the proliferation of the cancer cells, we performed Apo-ONE Homogeneous Caspase-3/7 assays. Caspase-3 and -7 are effector caspases that execute cell apoptosis via cleaving relevant cellular substrates (46). The negative effect of miR-183-5p on caspase-3/7 activity indicated that the knockdown of miR-183-5p caused apoptosis of LUAD cells. Therefore, we hypothesized that miR-183-5p may accelerate the malignant progression of LUAD by

enhancing tumor growth and inhibiting tumor apoptosis. It was discovered in previous studies that miR-183-5p modulated the expression of tumor-suppressor genes such as PDCD4 and SOCS-6 to accelerate the proliferation of cancer cells (47,48). In an *in vitro* experiment by Yan *et al*, the reduced cell growth and increased cell apoptosis by miR-183-5p inhibitor was correlated with upregulated caspase-3 and downregulated anti-apoptotic protein BCL-xl (43). These findings might provide interpretation of how miR-183-5p contributed to cell growth and suppressed cell apoptosis in LUAD.

In order to develop effective therapeutic and diagnostic targets for LUAD, it is not sufficient to merely identify the relationship between miR-183-5p expression and the malignant properties of LUAD. Therefore, we further attempted to explore the underlying molecular basis of the cell growth-promoting effects of miR-183-5p in LUAD via *in silico* analysis of miR-183-5p target genes. The significant terms identified from the GO analysis including positive regulation of gene expression, cell adhesion, actin filament organization, Ras guanyl-nucleotide exchange factor activity, glycosaminoglycan binding and calcium ion binding imply that target genes regulated by miR-183-5p may participate in these biological functions to cause the occurrence and development of LUAD. We can also draw conclusions from the KEGG pathway analysis. Among all the listed KEGG pathways significantly identified by analysis of the target genes of miR-183-5p, we noted that the top two pathways, CAMs and pathways in cancer, were closely associated with the formation of human cancers. CAMs are cell surface proteins that mediate the adhesion between cells and the extracellular matrix. This feature allows CAMs to stimulate the motility, invasion and angiogenesis of tumor cells (49,50). We speculate that miR-183-5p may target downstream CAMs to contribute to the progression of LUAD. Apart from CAMs and pathways in cancer, other pathways, such as endocytosis and axon guidance, were also identified as significantly enriched by analysis of the target genes of miR-183-5p. Involvement of target genes in these additional pathways may have an impact on LUAD; this awaits further study. In addition to the above results, we noted from DO analysis that the target genes were significantly assembled in chronic pulmonary heart disease and primary pulmonary hypertension, the function of target genes in chronic pulmonary heart disease and primary pulmonary hypertension may constitute part of the pathogenesis of LUAD.

Although the regulatory network of target genes was intricate, we focused on hub genes to shed light on the molecular mechanism of miR-183-5p in LUAD. Ten genes were screened out as hub genes from the four most significant KEGG pathways. However, several of the hub genes including *CD34*, *PDGFB*, *FGFR2* and *WNT3A* were described in previous studies to relate to the tumorigenesis or poor prognosis of LUAD (51-54). Although there have not been studies investigating the expression of *SPN*, *WNT2B* and *PTGER4* in LUAD, all the three genes were reported to act as an oncogene in other cancers. SPN could induce cell adhesion and migration as well as suppress apoptosis when secreted by activated leukocytes (55). WNT2B controlled multiple biological events, including cell proliferation, differentiation and migration to serve as an oncogene in numerous human cancers (56-58). PTGER4 could transduce a series of signaling pathways such as Akt, ERK1/2 and early growth response factor-1 to mediate cancer cell survival and tumor development with its overexpression in a wide variety of cancers (59). Thus, we are skeptical about the regulatory targeting relationship between miR-183-5p and these genes. Whether these genes were the direct targets of miR-183-5p needs to be verified in future study. Apart from these genes, we found evidence that VIPR1 was downregulated in LUAD and served as a tumor-suppressor gene in the study of Mlakar *et al* (60), which lend credence to the assumption that miR-183-5p directly targets VIPR1. In addition to the hub genes, component genes in CAMs pathway validated by Pearson's correlation test and immunostaining results from HPA were also worthy for attention. Despite that we found no literature evidence of the downregulation of expression in LUAD for all component genes in the CAMs pathway, the tumor suppressor roles of *SIGLEC1* and *CADM1* human cancers were explored in previous research. The study conducted by Strömvall *et al* confirmed that reduced expression of SIGLEC1 in metastasis-free regional lymph nodes was responsible for the inhibited antitumor immune response (61). CADM1, a membrane-spanning glycoprotein that participates in the process of attenuating cell proliferation and activating cell apoptosis, was downregulated in various cancers such as breast, prostate, pancreatic and hepatocellular cancer (62). We believe that miR-183-5p-regulated downexpression of genes such as *VIPR1*, *SIGLEC1* and *CADM1* may help explain the oncogenic function of miR-183-5p in LUAD. Future experiments are warranted to identify the interactions between miR-183-5p and these genes in LUAD.

Despite the research progress in our study, there were also limitations. In our GEO and integrated meta-analysis, great heterogeneity existed in the pooled studies, and even the subgroup analysis or sensitivity analysis failed to solve the problem, which unfortunately impacts the reliability of our results. This intractable heterogeneity may partly be attributed to the different proportion of LUAD and non-cancer tissues in the studies or the varying experimental platforms of studies. The number of LUAD tissues exceeded non-cancer tissues in GSE27486, GSE93300, GSE14936, GSE48414, GSE51853, GSE63805, GSE74190 and the TCGA data; conversely, the cases of non-cancer tissues outnumbered LUAD tissues in GSE19945, GSE40738, GSE47525 and GSE77380. The experimental platforms of studies also varied from each other. A feasible way to prevent this problem may be to enroll larger study cohorts with a balanced proportion of LUAD and non-cancer tissues in future studies. Another flaw of this study was that neither western blotting nor flow cytometry was conducted in *in vitro* experiments. Western blotting and flow cytometry should be conducted after knockdown or overexpression of miR-183-5p in the LC cell lines. Nevertheless, we failed to perform western blotting and flow cytometry due to the restriction of the experimental condition. This imperfect design of the *in vitro* experiment should be improved in future research.

In conclusion, our study confirmed that overexpression of miR-183-5p may play an oncogenic role in LUAD through involvement in the regulatory networks of its target genes. miR-183-5p is anticipated to be a novel diagnostic and therapeutic target for lung adenocarcinoma.

Acknowledgements

Not applicable.

Funding

The study was supported by funds from the National Natural Science Foundation of China (NSFC81560469, NSFC81360327), the Natural Science Foundation of Guangxi, China (2015GXNSFCA139009) and teh Guangxi Medical University Training Program for Distinguished Young Scholars (2017).

Availability of data and materials

The datasets generated and analysed during the current study are available in Gene Expression omnibus (GEO; https://www.ncbi.nlm.nih.gov/pubmed) and TCGA data portal (https://portal.gdc.cancer.gov/).

Authors' contributions

RQH and LG analyzed and interpreted data and drafted the manuscript. JM, ZYL, XHH and GC provided information from database. All authors read and approved the final manuscript.

Ethics approval and consent to participate

The study was approved by the Research Ethics Committee of the First Affiliated Hospital of Guangxi Medical University. Signed informed consents were acquired from all the LUAD patients prior to their involvement in this study.

Consent for publication

Not applicable.

Competing interests

The authors declare that they have no competing interests.

References

1. Siegel RL, Miller KD and Jemal A: Cancer Statistics, 2017. CA Cancer J Clin 67: 7-30, 2017.
2. Sharma SV, Bell DW, Settleman J and Haber DA: Epidermal growth factor receptor mutations in lung cancer. Nat Rev Cancer 7: 169-181, 2007.
3. Choi YL, Sun JM, Cho J, Rampal S, Han J, Parasuraman B, Guallar E, Lee G, Lee J and Shim YM: EGFR mutation testing in patients with advanced non-small cell lung cancer: A comprehensive evaluation of real-world practice in an East Asian tertiary hospital. PLoS One 8: e56011, 2013.
4. Cobo M, Gutiérrez V, Villatoro R, Trigo JM, Ramos I, López O, Ruiz M, Godoy A, López I and Arroyo M: Spotlight on ramucirumab in the treatment of nonsmall cell lung cancer: Design, development, and clinical activity. Lung Cancer (Auckl) 8: 57-66, 2017.
5. Yang Q, Zhang RW, Sui PC, He HT and Ding L: Dysregulation of non-coding RNAs in gastric cancer. World J Gastroenterol 21: 10956-10981, 2015.
6. Romero-Cordoba SL, Salido-Guadarrama I, Rodriguez-Dorantes M and Hidalgo-Miranda A: miRNA biogenesis: Biological impact in the development of cancer. Cancer Biol Ther 15: 1444-1455, 2014.
7. Mulrane L, McGee SF, Gallagher WM and O'Connor DP: miRNA dysregulation in breast cancer. Cancer Res 73: 6554-6562, 2013.
8. Palanichamy JK and Rao DS: miRNA dysregulation in cancer: Towards a mechanistic understanding. Front Genet 5: 54, 2014.
9. Wang H, Guan X, Tu Y, Zheng S, Long J, Li S, Qi C, Xie X, Zhang H and Zhang Y: MicroRNA-29b attenuates non-small cell lung cancer metastasis by targeting matrix metalloproteinase 2 and PTEN. J Exp Clin Cancer Res 34: 59, 2015.
10. Dambal S, Shah M, Mihelich B and Nonn L: The microRNA-183 cluster: The family that plays together stays together. Nucleic Acids Res 43: 7173-7188, 2015.
11. Chen H, Zhang L, Zhang L, Du J, Wang H and Wang B: MicroRNA-183 correlates cancer prognosis, regulates cancer proliferation and bufalin sensitivity in epithelial ovarian caner. Am J Transl Res 8: 1748-1755, 2016.
12. Cheng Y, Xiang G, Meng Y and Dong R: MiRNA-183-5p promotes cell proliferation and inhibits apoptosis in human breast cancer by targeting the PDCD4. Reprod Biol 16: 225-233, 2016.
13. Fan D, Wang Y, Qi P, Chen Y, Xu P, Yang X, Jin X and Tian X: MicroRNA-183 functions as the tumor suppressor via inhibiting cellular invasion and metastasis by targeting MMP-9 in cervical cancer. Gynecol Oncol 141: 166-174, 2016.
14. Xu F, Zhang H, Su Y, Kong J, Yu H and Qian B: Up-regulation of microRNA-183-3p is a potent prognostic marker for lung adenocarcinoma of female non-smokers. Clin Transl Oncol 16: 980-985, 2014.
15. Zhu WY, Zhang YK, Chai Z, Hu X, Tan L, Wang Z, Chen Z and Le H: Identification of factors for the preoperative prediction of tumour subtype and prognosis in patients with T1 lung adenocarcinoma. Dis Markers 2016: 9354680, 2016.
16. Zhu C, Deng X, Wu J, Zhang J, Yang H, Fu S, Zhang Y, Han Y, Zou Y, Chen Z, *et al*: MicroRNA-183 promotes migration and invasion of CD133(+)/CD326(+) lung adenocarcinoma initiating cells via PTPN4 inhibition. Tumour Biol 37: 11289-11297, 2016.
17. Higgins JP, Thompson SG, Deeks JJ and Altman DG: Measuring inconsistency in meta-analyses. BMJ 327: 557-560, 2003.
18. Harbord RM, Deeks JJ, Egger M, Whiting P and Sterne JA: A unification of models for meta-analysis of diagnostic accuracy studies. Biostatistics 8: 239-251, 2007.
19. Chen G, Kronenberger P, Teugels E and De Grève J: Influence of RT-qPCR primer position on EGFR interference efficacy in lung cancer cells. Biol Proced Online 13: 1, 2010.
20. Chen G, Noor A, Kronenberger P, Teugels E, Umelo IA and De Grève J: Synergistic effect of afatinib with su11274 in non-small cell lung cancer cells resistant to gefitinib or erlotinib. PLoS One 8: e59708, 2013.
21. Chen G, Umelo IA, Lv S, Teugels E, Fostier K, Kronenberger P, Dewaele A, Sadones J, Geers C and De Grève J: miR-146a inhibits cell growth, cell migration and induces apoptosis in non-small cell lung cancer cells. PLoS One 8: e60317, 2013.
22. Tang R, Zhong T, Dang Y, Zhang X, Li P and Chen G: Association between downexpression of MiR-203 and poor prognosis in non-small cell lung cancer patients. Clin Transl Oncol 18: 360-368, 2016.
23. Huang S, He R, Rong M, Dang Y and Chen G: Synergistic effect of MiR-146a mimic and cetuximab on hepatocellular carcinoma cells. Biomed Res Int 2014: 384121, 2014.
24. Dang YW, Zeng J, He RQ, Rong MH, Luo DZ and Chen G: Effects of miR-152 on cell growth inhibition, motility suppression and apoptosis induction in hepatocellular carcinoma cells. Asian Pac J Cancer Prev 15: 4969-4976, 2014.
25. Dang Y, Luo D, Rong M and Chen G: Underexpression of miR-34a in hepatocellular carcinoma and its contribution towards enhancement of proliferating inhibitory effects of agents targeting c-MET. PLoS One 8: e61054, 2013.
26. Rong M, Chen G and Dang Y: Increased miR-221 expression in hepatocellular carcinoma tissues and its role in enhancing cell growth and inhibiting apoptosis in vitro. BMC Cancer 13: 21, 2013.
27. Liang HW, Ye ZH, Yin SY, Mo WJ, Wang HL, Zhao JC, Liang GM, Feng ZB, Chen G and Luo DZ: A comprehensive insight into the clinicopathologic significance of miR-144-3p in hepatocellular carcinoma. Onco Targets Ther 10: 3405-3419, 2017.
28. Uhlén M, Fagerberg L, Hallström BM, Lindskog C, Oksvold P, Mardinoglu A, Sivertsson Å, Kampf C, Sjöstedt E, Asplund A, *et al*: Proteomics. Tissue-based map of the human proteome. Science 347: 1260419, 2015.
29. Patnaik SK, Yendamuri S, Kannisto E, Kucharczuk JC, Singhal S and Vachani A: MicroRNA expression profiles of whole blood in lung adenocarcinoma. PLoS One 7: e46045, 2012.

30. Patnaik SK, Kannisto ED, Mallick R, Vachani A and Yendamuri S: Whole blood microRNA expression may not be useful for screening non-small cell lung cancer. PLoS One 12: e0181926, 2017.
31. Seike M, Goto A, Okano T, Bowman ED, Schetter AJ, Horikawa I, Mathe EA, Jen J, Yang P, Sugimura H, *et al*: MiR-21 is an EGFR-regulated anti-apoptotic factor in lung cancer in never-smokers. Proc Natl Acad Sci USA 106: 12085-12090, 2009.
32. Nymark P, Guled M, Borze I, Faisal A, Lahti L, Salmenkivi K, Kettunen E, Anttila S and Knuutila S: Integrative analysis of microRNA, mRNA and aCGH data reveals asbestos- and histology-related changes in lung cancer. Genes Chromosomes Cancer 50: 585-597, 2011.
33. van Jaarsveld MT, Wouters MD, Boersma AW, Smid M, van Ijcken WF, Mathijssen RH, Hoeijmakers JH, Martens JW, van Laere S, Wiemer EA, *et al*: DNA damage responsive microRNAs misexpressed in human cancer modulate therapy sensitivity. Mol Oncol 8: 458-468, 2014.
34. Bjaanaes MM, Halvorsen AR, Solberg S, Jørgensen L, Dragani TA, Galvan A, Colombo F, Anderlini M, Pastorino U, Kure E, *et al*: Unique microRNA-profiles in EGFR-mutated lung adenocarcinomas. Int J Cancer 135: 1812-1821, 2014.
35. Arima C, Kajino T, Tamada Y, Imoto S, Shimada Y, Nakatochi M, Suzuki M, Isomura H, Yatabe Y, Yamaguchi T, *et al*: Lung adenocarcinoma subtypes definable by lung development-related miRNA expression profiles in association with clinicopathologic features. Carcinogenesis 35: 2224-2231, 2014.
36. Robles AI, Arai E, Mathé EA, Okayama H, Schetter AJ, Brown D, Petersen D, Bowman ED, Noro R, Welsh JA, *et al*: An integrated prognostic classifier for stage I lung adenocarcinoma based on mRNA, microRNA, and DNA methylation biomarkers. J Thorac Oncol 10: 1037-1048, 2015.
37. Ma L, Huang Y, Zhu W, Zhou S, Zhou J, Zeng F, Liu X, Zhang Y and Yu J: An integrated analysis of miRNA and mRNA expressions in non-small cell lung cancers. PLoS One 6: e26502, 2011.
38. Peng Z, Pan L, Niu Z, Li W, Dang X, Wan L, Zhang R and Yang S: Identification of microRNAs as potential biomarkers for lung adenocarcinoma using integrating genomics analysis. Oncotarget 8: 64143-64156, 2017.
39. Pak MG, Lee CH, Lee WJ, Shin DH and Roh MS: Unique microRNAs in lung adenocarcinoma groups according to major TKI sensitive EGFR mutation status. Diagn Pathol 10: 99, 2015.
40. Tanaka M, Oikawa K, Takanashi M, Kudo M, Ohyashiki J, Ohyashiki K and Kuroda M: Down-regulation of miR-92 in human plasma is a novel marker for acute leukemia patients. PLoS One 4: e5532, 2009.
41. Ohyashiki K, Umezu T, Yoshizawa S, Ito Y, Ohyashiki M, Kawashima H, Tanaka M, Kuroda M and Ohyashiki JH: Clinical impact of down-regulated plasma miR-92a levels in non-Hodgkin's lymphoma. PLoS One 6: e16408, 2011.
42. Shigoka M, Tsuchida A, Matsudo T, Nagakawa Y, Saito H, Suzuki Y, Aoki T, Murakami Y, Toyoda H, Kumada T, *et al*: Deregulation of miR-92a expression is implicated in hepatocellular carcinoma development. Pathol Int 60: 351-357, 2010.
43. Yan D, Cai X and Feng Y: miR-183 modulates cell apoptosis and proliferation in tongue squamous cell carcinoma SCC25 cell line. Oncol Res 24: 399-404, 2016.
44. Ruan H, Liang X, Zhao W, Ma L and Zhao Y: The effects of microRNA-183 promots cell proliferation and invasion by targeting MMP-9 in endometrial cancer. Biomed Pharmacother 89: 812-818, 2017.
45. Wang X, Zuo D, Yuan Y, Yang X, Hong Z and Zhang R: MicroRNA-183 promotes cell proliferation via regulating programmed cell death 6 in pediatric acute myeloid leukemia. J Cancer Res Clin Oncol 143: 169-180, 2017.
46. Cui R, Kim T, Fassan M, Meng W, Sun HL, Jeon YJ, Vicentini C, Tili E, Peng Y, Scarpa A, *et al*: MicroRNA-224 is implicated in lung cancer pathogenesis through targeting caspase-3 and caspase-7. Oncotarget 6: 21802-21815, 2015.
47. Miao F, Zhu J, Chen Y, Tang N, Wang X and Li X: MicroRNA-183-5p promotes the proliferation, invasion and metastasis of human pancreatic adenocarcinoma cells. Oncol Lett 11: 134-140, 2016.
48. Ren LH, Chen WX, Li S, He XY, Zhang ZM, Li M, Cao RS, Hao B, Zhang HJ, Qiu HQ, *et al*: MicroRNA-183 promotes proliferation and invasion in oesophageal squamous cell carcinoma by targeting programmed cell death 4. Br J Cancer 111: 2003-2013, 2014.
49. Makrilia N, Kollias A, Manolopoulos L and Syrigos K: Cell adhesion molecules: Role and clinical significance in cancer. Cancer Invest 27: 1023-1037, 2009.
50. Henderson MP, Hirte H, Hotte SJ and Kavsak PA: Cytokines and cell adhesion molecules exhibit distinct profiles in health, ovarian cancer, and breast cancer. Heliyon 2: e00059, 2016.
51. Kaseda K, Ishii G, Aokage K, Takahashi A, Kuwata T, Hishida T, Yoshida J, Kohno M, Nagai K and Ochiai A: Identification of intravascular tumor microenvironment features predicting the recurrence of pathological stage I lung adenocarcinoma. Cancer Sci 104: 1262-1269, 2013.
52. Xu J, Lv W, Hu Y, Wang L, Wang Y, Cao J and Hu J: Wnt3a expression is associated with epithelial-mesenchymal transition and impacts prognosis of lung adenocarcinoma patients. J Cancer 8: 2523-2531, 2017.
53. Timsah Z, Berrout J, Suraokar M, Behrens C, Song J, Lee JJ, Ivan C, Gagea M, Shires M, Hu X, *et al*: Expression pattern of FGFR2, Grb2 and Plcγ1 acts as a novel prognostic marker of recurrence recurrence-free survival in lung adenocarcinoma. Am J Cancer Res 5: 3135-3148, 2015.
54. Neri S, Miyashita T, Hashimoto H, Suda Y, Ishibashi M, Kii H, Watanabe H, Kuwata T, Tsuboi M, Goto K, *et al*: Fibroblast-led cancer cell invasion is activated by epithelial-mesenchymal transition through platelet-derived growth factor BB secretion of lung adenocarcinoma. Cancer Lett 395: 20-30, 2017.
55. Fu Q, Cash SE, Andersen JJ, Kennedy CR, Madadi AR, Raghavendra M, Dietrich LL, Agger WA and Shelley CS: Intracellular patterns of sialophorin expression define a new molecular classification of breast cancer and represent new targets for therapy. Br J Cancer 110: 146-155, 2014.
56. Jiang H, Li F, He C, Wang X, Li Q and Gao H: Expression of Gli1 and Wnt2B correlates with progression and clinical outcome of pancreatic cancer. Int J Clin Exp Pathol 7: 4531-4538, 2014.
57. Liu C, Li G, Ren S, Su Z, Wang Y, Tian Y, Liu Y and Qiu Y: miR-185-3p regulates the invasion and metastasis of nasopharyngeal carcinoma by targeting WNT2B in vitro. Oncol Lett 13: 2631-2636, 2017.
58. Clevers H and Nusse R: Wnt/β-catenin signaling and disease. Cell 149: 1192-1205, 2012.
59. Catalano RD, Wilson MR, Boddy SC, McKinlay AT, Sales KJ and Jabbour HN: Hypoxia and prostaglandin E receptor 4 signalling pathways synergise to promote endometrial adenocarcinoma cell proliferation and tumour growth. PLoS One 6: e19209, 2011.
60. Mlakar V, Strazisar M, Sok M and Glavac D: Oligonucleotide DNA microarray profiling of lung adenocarcinoma revealed significant downregulation and deletions of vasoactive intestinal peptide receptor 1. Cancer Invest 28: 487-494, 2010.
61. Strömvall K, Sundkvist K, Ljungberg B, Halin Bergström S and Bergh A: Reduced number of $CD169^+$ macrophages in pre-metastatic regional lymph nodes is associated with subsequent metastatic disease in an animal model and with poor outcome in prostate cancer patients. Prostate 77: 1468-1477, 2017.
62. Wikman H, Westphal L, Schmid F, Pollari S, Kropidlowski J, Sielaff-Frimpong B, Glatzel M, Matschke J, Westphal M, Iljin K, *et al*: Loss of CADM1 expression is associated with poor prognosis and brain metastasis in breast cancer patients. Oncotarget 5: 3076-3087, 2014.